Austrian Journal of Earth Sciences | Vienna | 2015 | Volume 108/2 | 219 - 238 | DOI: 10.17738/ajes.2015.0023

Polyphase metamorphism at the southeastern margin of the Graz Paleozoic and the underlying Austroalpine basement units

Philip SCHANTL[1)*)], Ralf SCHUSTER[2)], Kurt KRENN[1)] & Georg HOINKES[1)]

[1)] Institute of Earth Sciences, University of Graz, Universitätsplatz 2, A-8010 Graz, Austria;

[2)] Geologische Bundesanstalt, Neulinggasse 38, A-1030 Wien, Austria;

[*)] Corresponding author, philip.schantl@edu.uni-graz.at

KEYWORDS Polymetamorphism; metamorphic zoning; geochronology; Graz Paleozoic; Anger Crystalline Unit

Abstract

This study presents new petrological data and Rb-Sr biotite ages from the southeastern margin of the Graz Paleozoic and the underlying complexes of the Anger Crystalline Unit. Recent mapping of the area constrains a new tectonic and lithostratigraphic subdivision. Some new lithostratigraphic units containing metapelites were introduced, and their metamorphic evolution is described here for the first time. In the investigated area the Graz Paleozoic is subdivided from top to bottom into the Gschnaidt Nappe with the Glöselhof Lithodeme at its base, the Schöckel Nappe with the Hirschkogel Lithodeme in the uppermost position and the lowermost Gasen Nappe. The Anger Crystalline Unit below is formed by the Rossegg and Rappold complexes comprising nappes of the Koralpe-Wölz Nappe System.

The distribution of index minerals exhibits a complex pattern. Textures and chemical zoning of garnets indicate a polymetamorphic evolution of the Glöselhof Lithodeme, Rossegg Complex and Rappold Complex. The whole nappe pile shows an Eoalpine (Cretaceous) metamorphic imprint with an inverted metamorphic field gradient in the Graz Paleozoic and an upright zoning in the Anger Crystalline Unit. For the Glöselhof Lithodeme temperatures of more than 510°C are estimated. The previous imprint in the complexes of the Anger Crystalline Unit is Permian in age, whereas the Glöselhof Lithodeme may be related to the Variscan or Permian event. In the Graz Paleozoic nappe stack, heating and cooling occurred in the Early Cretaceous. In contrast, in the Anger Crystalline Unit and Koralpe-Wölz Nappe System respectively, a metamorphic peak in the early Late Cretaceous (Turonian) was followed by cooling until the end of Late Cretaceous (Campanian). The inverted and upright field gradient in combination with the different timing of metamorphism in the Graz Paleozoic and the Anger Crystalline Unit indicates a major Eoalpine thrust in between.

In der vorliegenden Arbeit werden petrologische Daten und Rb-Sr Glimmeralter vom südöstlichen Rand des Grazer Paläozoikums und den darunterliegenden Komplexen des sogenannten Angerkristallins präsentiert. Die Neukartierung des Gebietes in den letzten Jahren erforderte eine Modifizierung der tektonischen und lithostratigraphischen Einteilung. Einige lithostratigraphische Einheiten wurden neu eingeführt und deren metamorphe Entwicklung wird an dieser Stelle erstmals beschrieben. Der südöstliche Rand des Grazer Paläozoikums wird vom Hangenden ins Liegende durch die Basis der Gschnaidt-Decke, dem Glöselhof-Lithodem, die Schöckel-Decke mit dem im Hangenden auftretenden Hirschkogel-Lithodem und die Gasen-Decke aufgebaut. Das darunterliegende Angerkristallin wird vom Rossegg- und Rappold-Komplex aufgebaut, welche jeweils eine Decke des Koralpe-Wölz-Deckensystem repräsentieren.

Das Auftreten der Indexminerale zeichnet sich durch ein komplexes Verteilungsmuster aus. Zudem implizieren die chemischen Granatzonierungen eine polymetamorphe Geschichte für das Glöselhof-Lithodem sowie für den Rossegg- und Rappold-Komplex. Der gesamte Deckenstapel ist durch eine eoalpidische (kretazische) Metamorphose gekennzeichnet. Dieser Stapel zeigt im Grazer Paläozoikum gegen das Hangende zunehmende Metamorphosebedingungen, während im Angerkristallin eine gegen das Liegende zunehmende Metamorphose festzustellen ist. Für das Glöselhof-Lithodem wurden Temperaturen von mehr als 510°C ermittelt. Die ältere Metamorphoseprägung im Angerkristallin erfolgte im Perm, im Glöselhof-Lithodem des Grazer Paläozoikums ist sie dem permischen oder variszischen Ereignis zuzuordnen.

Die Deckenstapelung, Metamorphose und Abkühlung geschah im Grazer Paläozoikum während der Unterkreide. Im Gegensatz dazu liegt der Metamorphosehöhepunkt im Angerkristallin bzw. im Koralpe-Wölz-Deckensystem in der frühen Oberkreide (Turonium) und die Abkühlung erfolgte in der späten Oberkreide (Campanium).

Die Metamorphosezonierung und der zeitlich unterschiedliche Metamorphoseverlauf implizieren, dass zwischen dem Grazer Paläozoikum und dem Angerkristallin eine eoalpidische Deckengrenze vorhanden ist.

1. Introduction

This work presents petrological and structural data on the south-easternmost part of the Paleozic of Graz (GP) and underlying crystalline complexes, formally described as "Angerkristallin" (Schwinner, 1925, 1935; Flügel and Maurin, 1958) and referred as Anger Crystalline Unit (ACU) in the following (Fig. 1). The relation of the GP and ACU is under discussion

for a long time. In the interpretation by Tollmann (1963) the contact between the GP and ACU represents a major thrust separating the Upper and Middle Austroalpine Units. In contrast, Flügel and Neubauer (1984) argued for a primary stratigraphic contact whereby both units belong to the Upper Austroalpine Unit. With respect to the nomenclature of Schmid et al. (2004), the GP belongs to the Drauzug-Gurktal Nappe System representing the structurally uppermost part of the Upper Austroalpine Unit, whereas the crystalline complexes below, including the ACU, are part of the Koralpe-Wölz Nappe System of the Upper Austroalpine Unit.

On the basis of recent mapping (Matura and Schuster, 2014), in combination with petrological and geochronological investigations (Röggla, 2007; Schantl and Brandner, 2013) a new and more detailed lithostratigraphic (lithodemic) and tectonic subdivision was established for the area discussed in here. This paper characterises metapelites from the Hirschkogel Lithodeme of the Schöckel Nappe, the Glöselhof Lithodeme of the Gschnaidt Nappe, and the Rappold and Rossegg complexes of the Koralpe-Wölz Nappe System (Fig. 2). The results bear important implications for the relation of the GP to the ACU.

2. Geological setting

The Graz Paleozoic is a 30 x 50 km-sized nappe stack, which is located to the north of Graz and consists of very low- to low-grade metamorphic Paleozoic sediments and metavolca-

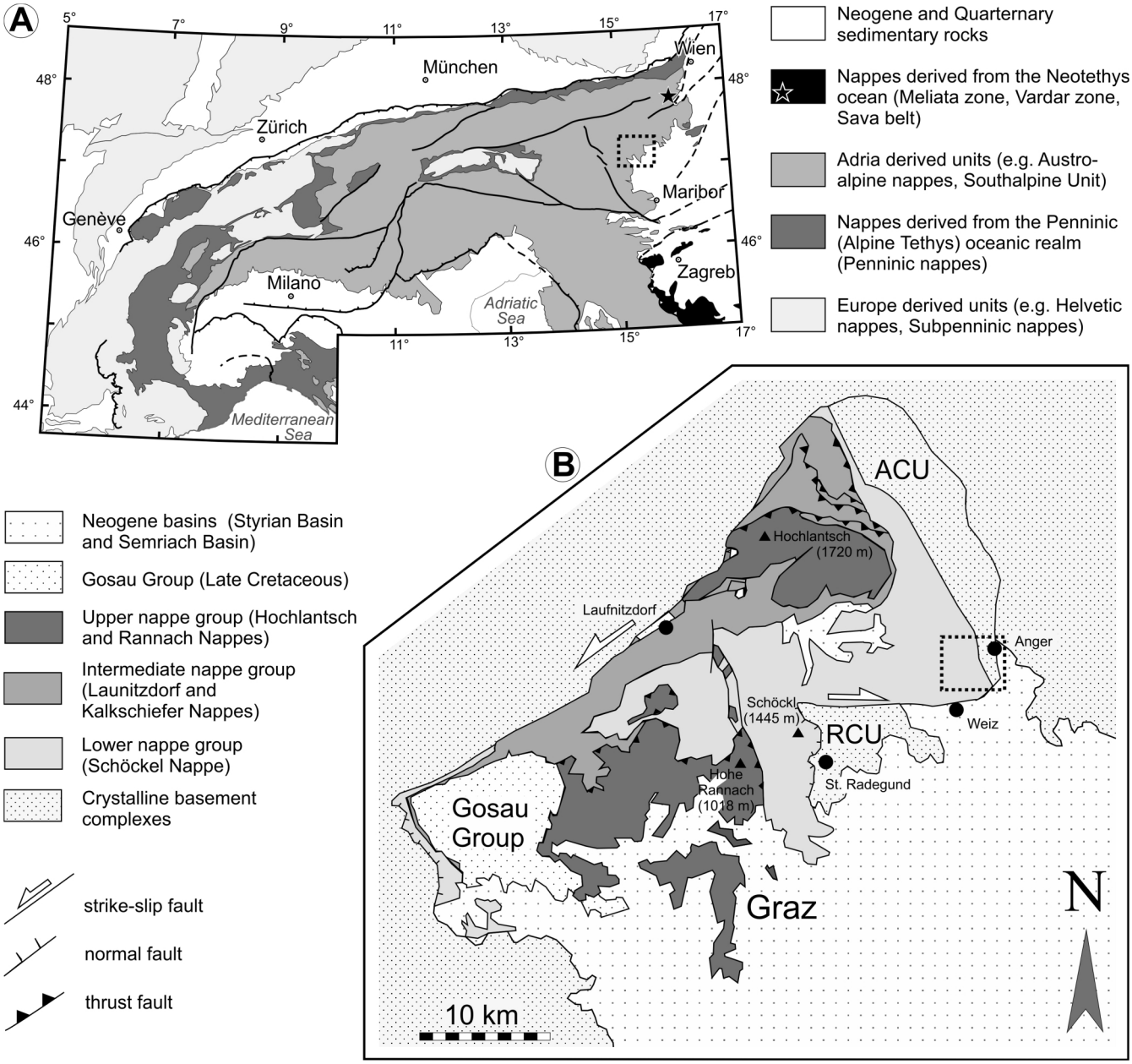

Figure 1: (A) Overview map indicating the paleogeographic origin of the main tectonic units of the Alps after Schmid et al. (2004). The dotted square indicates the position of the map shown in Figure 1B. (B) Geological sketch map of the Graz Paleozoic and the underlying crystalline complexes (modified after Krenn et al. 2008). The study area is indicated by the dotted square. ACU (Anger Crystalline Unit) and RCU (Radegund Crystalline Unit; not the same as Radegund Nappe!) are not tectonic nor lithostratigraphic terms, but describe local occurrences of metamorphosed rocks.

nics (Flügel and Neubauer, 1984; Fritz and Neubauer, 1988; Gasser et al., 2010). It is underlain by epidote-amphibolite facies to eclogite facies metamorphic units (Oberhänsli et al., 2004) such as the ACU and Radegund Crystalline Unit (RCU) (Figs. 1A, B). The western part of the GP is locally overlain by Upper Cretaceous sediments of the Gosau Group (Kainach-Subgroup) (Gräf, 1975; Ebner and Rantitsch, 2000), whereas to the south and close to Passail, the nappe stack is covered by Neogene sediments of the Styrian and Passail basins (Flügel and Neubauer, 1984; Fritz, 1988; Fritz et al., 1992; Gross et al., 2007).

The successions of the GP start with Early Silurian to Early Devonian volcanoclastics and siliciclastics, followed by Middle Devonian sediments of a carbonate platform. The sequence ends with pelagic limestones and slates of Late Devonian to Early Carboniferous age (Flügel and Neubauer, 1984; Fritz and Neubauer, 1988; Flügel and Hubmann, 2000; Gasser et al., 2010). Flügel and Hubmann (2000) described thirty-five for-

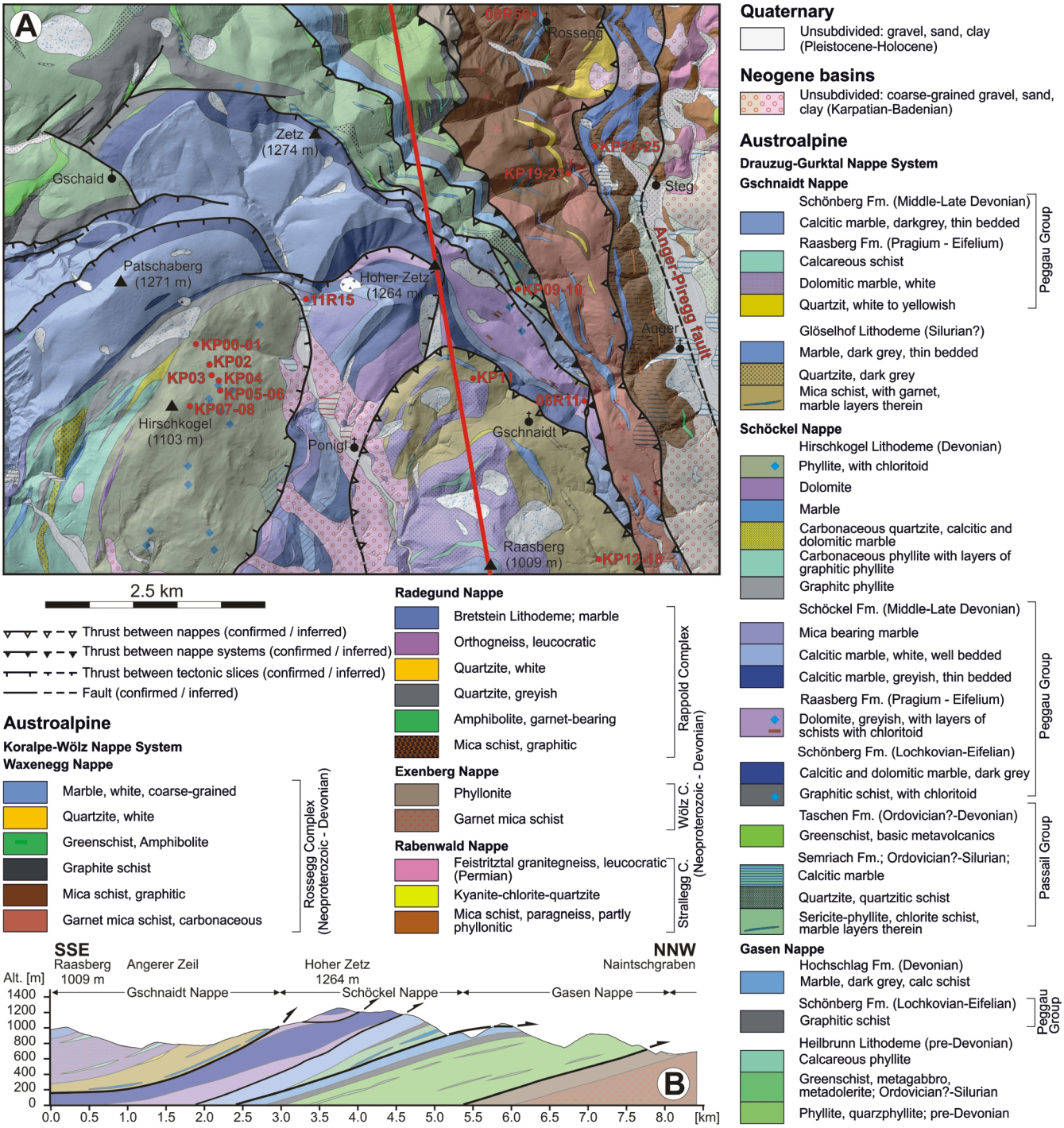

Figure 2: (A) Geological map of the study area after Matura and Schuster (2014). Sample localities are marked in red. The red line indicates the position of the section in Figure 2B. (B) Section through the lower nappe group of the Graz Paleozoic and the underlying crystalline complexes of the Anger Crystalline Unit.

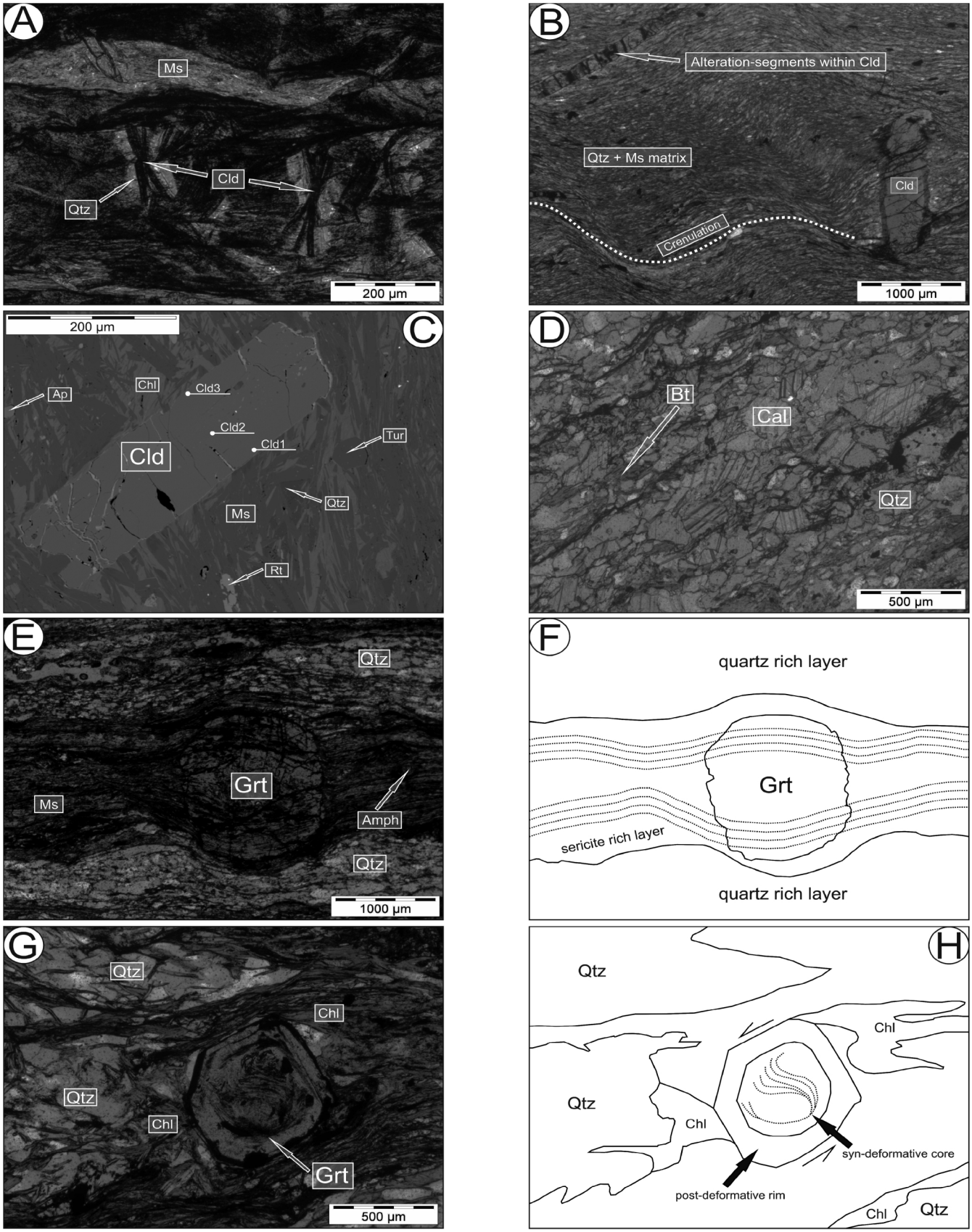

Amph, amphibole; Ap, apatite; Bt, biotite; Cal, calcite; Chl, chlorite; Cld, chloritoid; Grt, garnet; Ms, muscovite; Qtz, quartz; Rt, rutile; Tur, tourmaline

Figure 3: Petrography of the metapelites from the Hirschkogel Lithodeme (A-C) and Glöselhof Lithodeme (D-H): (A) chloritoid with typical radial habitus within a matrix composed of sericite and quartz; (B) chloritoid showing alteration segments embedded in a crenulated quartz-sericite-matrix; (C) BSE-image indicating the occurrence of chloritoid within the Hirschkogel Lithodeme as post-deformative porphyroblast and the measured points within chloritoid; (D) biotite and calcite-rich metapelite, showing typical twinning of calcite; (E, F) Synto post-deformative garnet within a sericite-rich layer surrounded by quartz-rich layers, the continuous transition between internal foliation and external foliation is visible; (G, H) garnet surrounded by retrograde chlorite and quartz, shows a syn-deformative core and a post-deformative rim.

Sample	Mineralogy	Latitude	Longitude	Unit	Nappe
KP11	Qtz, Ms, Bt, Chl, Cal, ±Ap, ±Rt, ±Tur, ±Zrn, ±Ilm, ±Py, ± graphitic	47°16'16.70"N	15°39'29.30"E	Glöselhof Lithodeme	Gschneidt Nappe/GP
KP12-KP18	Qtz, Ms, Grt, Zo, Bt, Chl, ±Ap, ±Rt, ±Tur, ±Zrn, ±Ilm, ± graphitic	47°15'06.10"N	15°40'40.40"E		
KP00-KP01	Qtz, Ms, Chl, Cld, ±Aln, ±Brt, ±Mnz, ±Ap, ±Rt, ±Tur, ±Zrn, ±Ilm, ± graphitic	47°16'19.43"N	15°37'09.10"E	Hirschkogel Lithodeme	Schöckel Nappe/GP
KP02-KP03		47°16'14.30"N	15°36'55.70"E		
KP04		47°16'09.80"N	15°36'59.10"E		
KP05-KP06		47°16'05.70"N	15°37'03.10"E		
KP07-KP08		47°16'03.80"N	15°37'02.10"E		
11R15	Cal, Qtz, Ms, Chl, ore phases, Zrn, Ap	47°16'46.70"N	15°37'52.70"E	Schöckel Formation	
08R11	Cal, Bt, Qtz, Ms, Zo, Chl, ore phases, Ap	47°16'07.50"N	15°40'32.90"E	Raasberg Formation	
KP09-KP10	Qtz, Ms, Bt, Chl, Cal,	47°16'48.07"N	15°39'54.80"E	Semriach Formation	
KP19-KP23	Qtz, Ms, Grt, ±Chl, Bt, ±Cld, ±Pl, ±Cal, ±Aln, ±Ap, ±Ep, ±Rt, ±Tur, ±Zrn, ±Ilm, ±Py	47°17'34.13"N	15°40'20.03"E	Rossegg Complex	Waxenegg Nappe/ACU
08R56	Ms, Qtz, Ab, Grt, Ilm, Zo, ±FeOOH, ± graphitic	47°18'37.50"N	15°40'04.50"E		
K24-KP25	Qtz, Ms, Grt, ±Chl, Bt, Pl, ±Aln, ±Rt, ±Tur, ±Zrn, ±Ilm, ± graphitic	47°17'42.84"N	15°40'34.15"E	Rappold Complex	Radegund Nappe/ACU
05R09	Qtz, Pl, Bt, Grt, Ms, ore phases, Ap	47°10'32.90"N	15°31'28.40"E		Radegund Crystalline Unit

Aln, allanite; Amph, amphibole; Ap, apatite; Brt, baryte; Bt, biotite; Cal, calcite; Chl, chlorite; Cld, chloritoid; Ep, epidote; Grt, garnet; Ilm, ilmenite; Mnz, monazite; Ms, muscovite; Pl, plagioclase; Py, pyrite; Qtz, quartz; Rt, rutile; Tur, tourmaline; Zo, zoisite; Zrn, zircon;

Table 1: Coordinates of the samples from the Graz Paleozoic, Anger Crystalline Unit and Radegund Crystalline Unit (see also Figure 2).

mations belonging to five different sedimentological facies units termed the Laufnitzdorf, Kalkschiefer, Schöckel, Rannach and Hochlantsch facies. After Flügel et al. (1990) and Fritz et al. (1992) these facies zones are found in three nappe groups: a lower Schöckel-, an intermediate Laufnitzdorf-Kalkschiefer- and an upper Rannach-Hochlantsch-nappe group.

However, the assignment of the individual nappes to the intermediate and lower nappe group is not unambiguous and therefore Gasser et al. (2010) introduced a subdivision of the GP into a lower and an upper nappe group (nappe system in Gasser et al. 2010) separated by the so called Rannach thrust. Recent mapping by Matura and Schuster (2014) revealed a more detailed subdivision of the lower nappe group in the easternmost part of the GP: from bottom to the top the nappe pile comprises the Gasen Nappe, Schöckel Nappe with the Hirschkogel Lithodeme in the stratigraphic uppermost position and the Gschnaidt Nappe including the mica schists of the Glöselhof Lithodeme at its base.

According to Gasser et al. (2010) the lower nappe group is characterised by a penetrative schistosity, isoclinal folds and an E–W trending stretching lineation. Deformation in the Rannach Thrust Zone is dominated by a stretching lineation that progressively turns from E–W to SE–NW. In both the lower and upper nappe group open folds with NE–SW trending fold axes occur (Krenn et al., 2008). Several brittle strike slip faults crosscut the GP and a potential metamorphic break respective normal fault between the lower nappe group and the Rannach nappe was mapped by Neubauer (1989). The GP is bordered by a normal fault in the west, a transtensional strike slip fault in the northwest and several complex strike slip, normal and thrust faults in the south and east (Fig. 1) (Fritz et al., 1992, Neubauer et al., 1995, Krenn et al., 2008).

Metamorphic conditions in the Paleozoic of Graz were studied by Hasenhüttl (1994), Russegger (1996), Rantitsch et al. (2005), and Krenn et al. (2008). In general sub-greenschist to lower-

Unit	Hirschkogel Lithodeme				Glöselhof L.		Rossegg Complex				Rappold C.	
Rock	Cld-phyllite				mica schist		Grt-mica schist		amphibolite		Grt-mica schist	
Sample	KP-01	KP-01	KP-02	KP-07	KP-11	KP-17	KP-19	KP-19	KP-22	KP-22	KP-24	KP-24
Data point	Ms 1	Ms 3	Ms 4	Ms 2	Ms 3	Ms 1	Ms 1	Ms 3	Ms 1	Ms 2	Ms 1	Ms 2
SiO_2	47.27	46.89	47.01	47.16	51.51	48.51	47.69	47.17	47.19	47.80	48.05	47.43
TiO_2	0.07	0.25	0.31	0.26	0.55	0.16	0.41	0.52	0.47	0.55	0.40	0.41
Al_2O_3	36.27	36.06	37.15	35.90	28.34	33.58	33.28	32.86	31.74	31.69	34.06	33.63
Cr_2O_3	0.02	0.00	0.00	0.06	0.01	0.11	0.03	0.02	0.05	0.07	0.00	0.05
CaO	0.04	0.02	0.00	0.00	0.01	0.01	0.00	0.00	0.00	0.00	0.03	0.00
FeO	0.82	1.25	0.98	1.34	1.48	1.57	2.71	2.95	3.10	3.15	1.57	1.53
MgO	0.56	0.44	0.00	0.31	3.17	1.32	1.48	1.26	1.30	1.34	1.17	1.14
MnO	0.00	0.00	0.00	0.00	0.00	0.00	0.00	0.00	0.00	0.00	0.00	0.00
K_2O	8.72	9.11	8.74	9.45	10.68	10.23	9.23	9.33	10.01	10.00	9.35	9.38
Na_2O	0.94	1.35	1.22	0.98	0.26	0.77	1.19	1.18	0.94	0.83	1.39	1.39
∑ [wt%]	94.72	95.38	95.41	95.46	96.04	96.26	96.02	95.28	94.80	95.43	96.02	94.96
Si	6.23	6.07	6.10	6.18	6.67	6.38	6.31	6.24	6.37	6.45	6.32	6.24
Ti	0.01	0.02	0.03	0.03	0.05	0.02	0.04	0.05	0.05	0.06	0.04	0.04
Al	5.64	5.50	5.68	5.55	4.33	5.20	5.19	5.12	5.05	5.04	5.28	5.21
Cr	0.00	0.00	0.00	0.01	0.00	0.01	0.00	0.00	0.01	0.01	0.00	0.01
Ca	0.01	0.00	0.00	0.00	0.00	0.00	0.00	0.00	0.00	0.00	0.00	0.00
Fe	0.09	0.14	0.11	0.15	0.16	0.17	0.30	0.33	0.35	0.36	0.17	0.17
Mg	0.11	0.09	0.00	0.06	0.61	0.26	0.29	0.25	0.26	0.27	0.23	0.22
MnO	0.00	0.00	0.00	0.00	0.00	0.00	0.00	0.00	0.00	0.00	0.00	0.00
K	1.47	1.51	1.45	1.58	1.76	1.72	1.56	1.57	1.72	1.72	1.57	1.57
Na	0.24	0.34	0.31	0.25	0.07	0.20	0.30	0.30	0.24	0.22	0.35	0.35
∑ Cat.	13.79	13.67	13.68	13.80	13.66	13.96	13.99	13.86	14.05	14.11	13.96	13.81

Table 2: Representative electron microscope analyses of selected muscovites of the Hirschkogel Lithodeme, Glöselhof Lithodeme, Rossegg Complex and Rappold Complex. Cations are calculated on the basis of 22 oxygens.

most greenschist facies conditions were determined for the Rannach-Hochlantsch nappe group and Laufnitzdorf nappes, whereas rocks of the Kalkschiefer and Schöckel nappes reached greenschist facies conditions.

There is a long discussion about the age of metamorphism and deformation within the GP. Based on different models the main imprint was attributed to the Variscan or Eoalpine (Cretaceous) tectonometamorphic event (Frank, 1981; Flügel et al., 1980; Esterlus, 1986; Fritz, 1988; Russegger 1996; Neubauer et al., 1999; Krenn et al., 2008). According to Fritz et al. (1992) an Eoalpine thrusting event at about 125 Ma is the major event, and most of the deformation in the GP took place during the Cretaceous.

The term Anger Crystalline Unit (ACU) is a local name for an area composed of metamorphic rocks located 30 km NE of Graz near to Anger (Fig. 1). It is overlain by the GP with a southwest dipping contact, whereas its eastern boundary towards other Austroalpine basement units of the Koralpe-Wölz Nappe System is a southwest dipping thrust, partly overprinted by a steeply dipping fault (Anger-Piregg fault). However, the ACU is neither a tectonic nor a lithostratigrahic unit. It consists of several metamorphic complexes forming nappes belonging to the Silvretta-Seckau and Koralpe-Wölz nappe systems, which also appear in the north and west of the GP in the Gleinalpe and Koralpe region (Schuster et al., 2014). Based on the map by Matura and Schuster (2014) the ACU can be subdivided into four complexes. The Rossegg Complex and the underlying Rappold Complex are described in the following chapters (Fig. 2).

The relation of the GP to the ACU is under discussion since a long time. In the early maps (Flügel and Maurin, 1958; Flügel, 1961, 1975) the boundary is uncertain, because it is only indicated by diffuse grids in some places. In contrast Tollmann (1963) argued for a major thrust between the crystalline basement and the Paleozoic sucessions. Quartzites and carbonate rocks at the Raasberg Mountain played a particular role, as they were thought to represent autochthonous Triassic sediments on top of the Middle Austroalpine unit, overlain by the Upper Austroalpine GP. Later on, Flügel and Neubauer (1984) argued for a continuous succession from the ACU into the GP and a pre-Alpine metamorphism sealing the nappe contact. The interpretation was based on two assumptions. Firstly, the marbles of the Hochschlag Formation and underlying light quartzites within black (graphitic) phyllites (Neubauer, 1981) were thought to continue from the GP into the ACU and secondly, a continuous downward increase of a pre-Alpine metamorphic imprint across the contact of the two units was postulated. This contact was overprinted by NE-directed shear zones followed by SW-trending normal faults during the Late Cretaceous (Krenn et al., 2008).

3. Analytical methods

3.1 Mineral chemistry

For quantitative mineral analyses a JEOL JSM 6310 electron microscope was used at the Institute of Earth Sciences, University of Graz. It is equipped with a Link Isis energydisper-sive X-ray (EDX) and a Microspec wave length-dispersive X-ray (WDX) spectrometer. Conditions of measurement were 15 kV acceleration voltage and 5 nA beam current. Natural and synthetic mineral standards were used for calibration. Mineral formulae were calculated using the program PET 7 (Dachs,

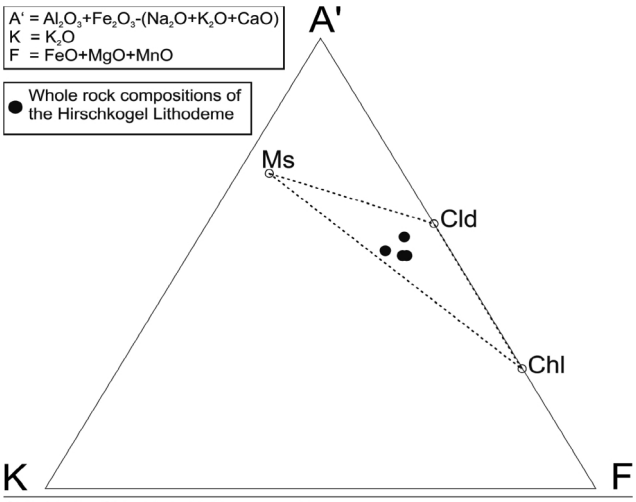

Chl, chlorite; Cld, chloritoid; Ms, muscovite

Figure 4: A'KF-projection showing whole rock compositions (based on analyses of Table 5) and measured mineral compositions of the muscovite-chloritoid-chlorite assemblage from the Hirschkogel Lithodeme.

Unit	Hirschkogel L.		Glöselhof L.		Rossegg C.		Rappold C.	
Rock	Cld-phyllite		mica schist		Grt-mica schist			
Sample	KP-07	KP-07	KP-14	KP-17	KP-19	KP-19	KP-24	KP-24
Data point	Chl 1	Chl 2	Chl 1	Chl 1	Chl 4	Chl 5	Chl 2	Chl 3
SiO_2	23.20	23.00	24.77	25.19	25.09	24.87	24.99	23.56
TiO_2	0.08	0.04	0.01	0.10	0.03	0.15	0.10	0.10
Al_2O_3	21.69	21.93	20.86	19.65	21.71	21.42	20.74	20.27
Cr_2O_3	0.04	0.00	0.06	0.06	0.00	0.02	0.00	0.04
CaO	0.05	0.03	0.13	0.11	0.00	0.00	0.03	0.04
FeO	33.43	34.00	26.94	27.48	25.44	26.39	29.63	28.69
MgO	6.10	6.64	12.29	12.25	13.70	13.17	11.39	11.23
MnO	0.11	0.02	0.03	0.17	0.09	0.12	0.10	0.11
Na_2O	n.d.	n.d.	n.d.	n.d.	n.d.	n.d.	n.d.	n.d.
K_2O	n.d.	n.d.	n.d.	n.d.	n.d.	n.d.	n.d.	n.d.
Σ [wt%]	84.70	85.66	85.09	85.01	86.06	86.14	86.98	84.04
Si	2.64	2.61	2.72	2.78	2.69	2.69	2.72	2.66
Ti	0.01	0.00	0.00	0.01	0.00	0.01	0.01	0.01
Al	2.91	2.94	2.70	2.55	2.75	2.73	2.66	2.70
Cr	0.00	0.00	0.00	0.00	0.00	0.00	0.00	0.00
Ca	0.01	0.00	0.02	0.01	0.00	0.00	0.00	0.01
Fe	3.18	3.23	2.47	2.53	2.28	2.38	2.70	2.71
Mg	1.04	1.12	2.01	2.01	2.19	2.12	1.85	1.89
Mn	0.01	0.00	0.00	0.02	0.01	0.01	0.01	0.01
Na	n.d.	n.d.	n.d.	n.d.	n.d.	n.d.	n.d.	n.d.
K	n.d.	n.d.	n.d.	n.d.	n.d.	n.d.	n.d.	n.d.
∑Cat.	9.79	9.91	9.92	9.92	9.92	9.93	9.94	9.98

Table 3: Representative electron microscope analyses of selected chlorites of the Hirschkogel Lithodeme, Glöselhof Lithodeme, Rossegg Complex and Rappold Complex. Cations are calculated on the basis of 14 oxygens.

1998) and NORM Version 4 (Ulmer, 1993, written comm.).

Major and trace elements of whole rocks were analysed by X-ray fluorescence (device designation: Bruker Pioneer S4) using powder pellets and the international standards. Mineral abbreviations were used after Kretz (1983).

3.2 Rb-Sr method

Mechanical and chemical sample preparation for Rb and Sr isotope analyses were performed at the Geological Survey of Austria in Vienna. Minerals were separated by standard methods of crushing, grinding, sieving and magnetic separations. Weights of samples used for dissolution were about 100 mg for whole rock powder and about 200 mg for micas. Chemical sample preparation follows the procedure described by Sölva et al. (2005). Isotopic measurements were done at the Department of Lithospheric Research at the University of Vienna. Rb and Sr concentrations were determined by isotope dilution using mixed Rb-Sr spikes. Rb ratios were measured with a Finnigan® MAT 262 MC-TIMS, whereas Sr ratios were analysed with a Thermo Finnigan® Triton MC-TIMS. Sr was run from Re double filaments, whereas Rb was evaporated from a Ta filament. Total procedural blanks are < 1ng for Rb and Sr. During the period of measurements the NBS987 standard yielded 86Sr/87Sr = 0.710248±4 (n=17; 2σm) on the Triton TI. Isochron ages were calculated with the software ISOPLOT/Ex (Ludwig, 2003) assuming an error of 1% on the 87Rb/86Sr ratio.

4. Description and results of investigated units

Samples from the GP were taken from the Hirschkogel Lithodeme (KP00-KP08), Schöckel Formation (11R15), Raasberg Formation (08R11), the Semriach Phyllite Formation (KP09-KP10) and from the Glöselhof Lithodeme (KP11-KP18). The ACU was sampled 2.5 km north of Anger, within the Rossegg Complex (KP19 to KP23, 08R59) and Rappold Complex (KP24 to KP25). One additional sample from the Rappold Complex was collected in the Radegund crystalline Unit (05R08). For sample locations see Figure 2 and Table 1.

Unit	Hirschkogel Lithodeme								Rossegg Complex			Rappold C.	
Rock	Cld-phyllite								Grt-mica schist				
Sample	KP-01	KP-01	KP-01	KP-01	KP-02	KP-02	KP-02	KP-02	KP-19	KP-19	KP-19	KP-24	KP-24
Data point	Cld1	Cld2	Cld4	Cld5	Cld1	Cld2	Cld3	Cld4	Cld1	Cld2	Cltd3	Cld1	Cld2
SiO_2	24.04	24.44	23.69	24.17	24.09	24.24	23.98	24.06	24.49	24.44	24.13	24.63	24.72
TiO_2	0.42	0.27	0.05	0.00	0.02	0.04	0.02	0.00	0.00	0.03	0.00	0.00	0.07
Al_2O_3	39.68	39.74	39.02	40.14	39.90	39.52	40.37	39.17	39.91	38.99	39.37	39.72	39.70
Cr_2O_3	0.07	0.03	0.10	0.00	0.09	0.07	0.09	0.05	0.01	0.09	0.00	0.04	0.09
CaO	0.00	0.02	0.02	0.00	0.02	0.00	0.03	0.00	0.04	0.06	0.01	0.08	0.03
FeO	25.05	24.88	25.72	23.94	24.89	25.32	25.14	24.81	24.50	24.71	24.50	24.11	25.11
MgO	1.90	2.30	2.21	2.41	2.21	1.63	2.13	1.64	2.68	2.53	2.89	2.59	1.89
MnO	0.74	0.62	0.54	0.57	0.84	0.76	0.80	0.83	0.30	0.40	0.02	0.08	0.22
K_2O	n.d.	n.d.	n.d.	n.d.	n.d.	n.d.	n.d.	n.d.	n.d.	n.d.	n.d.	n.d.	n.d.
Na_2O	n.d.	n.d.	n.d.	n.d.	n.d.	n.d.	n.d.	n.d.	n.d.	n.d.	n.d.	n.d.	n.d.
∑ [wt%]	91.90	92.30	91.35	91.23	92.06	91.58	92.56	90.56	91.93	91.25	90.92	91.25	91.83
Si	1.01	1.02	1.00	1.01	1.00	1.02	0.99	1.02	1.02	1.03	1.01	1.03	1.03
Ti	0.01	0.01	0.00	0.00	0.00	0.00	0.00	0.00	0.00	0.00	0.00	0.00	0.00
Al	1.96	1.95	1.93	1.98	1.96	1.96	1.97	1.96	1.95	1.93	1.95	1.95	1.95
Cr	0.00	0.00	0.00	0.00	0.00	0.00	0.00	0.00	0.00	0.00	0.00	0.00	0.00
CaO	0.00	0.00	0.00	0.00	0.00	0.00	0.00	0.00	0.00	0.00	0.00	0.00	0.00
Fe	0.88	0.87	0.91	0.84	0.87	0.89	0.87	0.88	0.86	0.87	0.86	0.84	0.88
Mg	0.12	0.14	0.14	0.15	0.14	0.10	0.13	0.10	0.17	0.16	0.18	0.16	0.12
Mn	0.03	0.02	0.02	0.02	0.03	0.03	0.03	0.03	0.01	0.01	0.00	0.00	0.01
K	n.d.	n.d.	n.d.	n.d.	n.d.	n.d.	n.d.	n.d.	n.d.	n.d.	n.d.	n.d.	n.d.
Na	n.d.	n.d.	n.d.	n.d.	n.d.	n.d.	n.d.	n.d.	n.d.	n.d.	n.d.	n.d.	n.d.
∑ Cat.	4.00	4.00	4.00	4.00	4.01	4.00	4.00	4.00	4.01	4.00	4.00	3.99	3.99

Table 4: Representative electron microscope analyses of selected chloritoids of the Hirschkogel Lithodeme, Rossegg Complex and Rappold Complex. Cations are calculated on the basis of 6 oxygens.

4.1 Hirschkogel Lithodeme (Schöckel Nappe/GP)

The type locality of the Hirschkogel Lithodem is at Hirschkogel (1103 m) 6 km north of Weiz. It is overlying the marbles of the Schöckel Formation and forms the stratigraphic top of the Schöckel Nappe. Its lower part consists of graphite-phyllites and carbonate bearing phyllites with intercalations of quartzites, quartzite rich carbonates, dolomite- and calcite marbles. The upper part is dominated by grey to silvery phyllites with sporadic appearance of chloritoid, which reach up to 2 mm in size. The thickness is a few hundred meters and it is expected to range from the late Middle Devonian to the Early Car-

Unit	Rock	Sample	SiO_2	TiO_2	Al_2O_3	CaO	Fe_2O_3	MgO	MnO	K_2O	Na_2O	P_2O_5	LOI	∑ [wt%]
Hirschkogel Lithodeme	Cld-phyllite	KP00	60.53	1.17	21.74	0.17	9.33	1.37	0.19	2.65	0.65	0.18	3.71	101.69
		KP02	54.25	1.22	23.90	0.12	9.87	2.14	0.21	4.09	0.67	0.17	4.99	101.64
		KP06	49.30	1.63	26.54	0.13	11.24	2.33	0.08	4.47	1.01	0.19	4.97	101.87
		KP07	53.36	1.30	24.36	0.00	10.50	1.12	0.06	5.05	0.65	0.16	4.86	101.41

Sample	Ba [ppm]	Ce	Cr	Cu	Ga	Nb	Nd	Ni	Pb	Rb	Sc	Sr	Th	U	V	Y	Zn	Zr
KP00	319	98	105	50	28	25	45	<20	28	139	22	192	<20	<20	130	38	112	193
KP02	585	106	112	42	33	25	51	54	24	191	23	158	25	<20	164	43	146	175
KP06	541	155	126	41	34	35	70	47	32	208	24	188	24	<20	195	51	152	248
KP07	808	69	116	60	32	25	66	54	26	232	23	132	21	<20	171	41	256	193

Table 5: Representative whole rock compositions of chloritoid-phyllites from the Hirschkogel Lithodeme.

boniferous (Schuster et al., 2014).

4.1.1 Petrography

In general, phyllites of the Hirschkogel Lithodeme contain sericite, quartz, chloritoid and chlorite. Apatite, rutile, tourmaline with graphitic inclusions, zircon, and rarely monazite, barite, ilmenite and allanite appear as accessories. Allanite is present only in sample KP01 as a single large grain 500 µm in diameter. White micas display a distinct schistosity which overprints the sedimentary layering. Chloritoid up to 2 mm in diameter is orientated either parallel or perpendicular to the schistosity and may occur as aggregates with radial habitus (Fig. 3A) showing typical twinning and alteration segments. Due to the orientation of chloritoid a syn- to post-deformative growth can be assumed. In addition, a distinctive crenulation cleavage is observed (Fig. 3B). White mica appears as very fine-grained sericite, but sometimes also larger post-deformative muscovite flakes occur. Fine-grained quartz shows partly undulose extinction.

4.1.2 Mineral- and whole rock chemistry

White mica is poor in Na_2O with an average value of 1.12 wt.% indicating low paragonite contents. The average of SiO_2 value is 47.08 wt.% and of FeO is 1.10 wt.% (Tab. 2).

Chlorite coexisting with chloritoid is rich in FeO with average values of 33.72 wt.% while the average MgO content is very low with about 6.37 wt.% (Tab. 3). The $Mg/(Mg+Fe_{tot})$ vs. Si plot after Bailey (1988) classifies chlorites of the Hirschkogel Lithodeme as chamosites.

Chloritoid occurs as syn- to post-deformative porphyroblasts (Fig. 3C). They represent chemically homogeneous Fe-chloritoides with approximately 25 wt.% FeO and 2.05 wt.% MgO (Tab. 4), resulting in high X_{Fe} of about 0.91. (Tab. 4).

The whole rock composition of the Hirschkogel Lithodeme indicates Al rich metapelites (Tab. 5). In the A´KF-diagram, whole rock compositions plot inside the measured mineral compositions of the divariant assemblage muscovite-chloritoid-chlorite (Fig. 4).

4.2 Glöselhof Lithodeme (Gschnaidt Nappe/GP)

The Glöselhof Lithodeme is present at the northern and eastern slopes of the Raasberg Mountain, forming the lowermost part of the Gschnaidt Nappe. The proposed type locality is at the collapsed mill in the gorge 500 m south of the farmhouse Glöselhof. The major rock types are fine-grained mica schists which are locally dominated by biotite or muscovite. The rocks show a dominant foliation which is partly overprinted by crenulation cleavage. Thin layers of dark grayish, fine-grained marble- and quartzites are intercalated (Schuster et al., 2014).

4.2.1 Petrography

Biotite dominated mica schists consist of quartz, calcite, biotite, sericite and accessories of apatite, monazite, rutile and zircon (Fig. 3D). Biotite shows zircon inclusions and pleochroic halos.

Muscovite dominated mica schists consist of muscovite, quartz, garnet, amphibole, biotite, (clino-) zoisite. The accessories are apatite, rutile, tourmaline, zircon and ilmenite. The amphiboles are pale green and normally less than 1 mm in size. Garnet is up to 1 mm in size and often idioblastic. Sometimes it forms poikiloblasts with inclusions of quartz or it contains fine-grained graphitic pigment. Some garnets are characterised by simple inclusion trails indicating a monophase evolution of the porphyroblasts (Fig. 3E, F), whereas others show cores growing syn-deformatively during simple shear deformation followed by static rim growth (Fig. 3G, H).

4.2.2 Mineral chemistry

White mica is classified as slightly phengitic muscovite with an average Si-content of 6.5 a.p.f.u. (Tab. 2).

Chlorite coexisting with almandine-rich garnet can be classified as chamosites by using the discriminating diagram after Bailey (1988) (Tab. 3). The higher content of MgO and lower content of FeO reflects the cation-exchange-reaction during garnet growth where the MgO content increases and the FeO content decreases in the phyllosilicates.

Biotite of the biotite dominated mica schists is classified

Unit	Glöselhof Lithodeme							
Rock	Bt dominated mica schist				Ms dominated mica schist			
Sample	KP-11	KP-11	KP-11	KP-11	KP-16	KP-17	KP-17	KP-17
Data point	Bt 1	Bt 2	Bt 5	Bt 6	Bt 2	Bt 1	Bt 2	Bt 4
SiO_2	38.30	37.56	38.83	38.92	37.48	35.71	35.79	35.77
TiO_2	1.44	1.35	1.46	1.51	2.05	2.14	2.20	2.19
Al_2O_3	16.67	16.90	16.05	16.44	17.59	17.40	18.10	16.76
Cr_2O_3	n.d.	n.d.	n.d.	n.d.	0.01	0.00	0.00	0.00
CaO	0.03	0.00	0.07	0.04	0.10	0.00	0.00	0.00
FeO	12.65	12.27	12.05	12.64	18.13	20.88	20.48	21.86
MgO	16.54	16.95	16.64	15.92	10.55	9.73	9.73	9.24
MnO	0.02	0.00	0.02	0.00	0.05	0.00	0.12	0.13
K_2O	9.65	9.37	9.71	9.78	7.60	8.36	8.87	8.85
Na_2O	n.d.	n.d.	n.d.	n.d.	n.d.	n.d.	n.d.	n.d.
F	0.55	0.50	0.73	0.71	n.d.	n.d.	n.d.	n.d.
Cl	0.11	0.06	0.10	0.07	n.d.	n.d.	n.d.	n.d.
∑ [wt%]	95.96	94.96	95.66	96.03	93.56	94.22	95.29	94.80
Si	2.84	2.80	2.90	2.91	2.89	2.78	2.77	2.80
Ti	0.08	0.08	0.08	0.08	0.12	0.13	0.13	0.13
Al	1.46	1.48	1.41	1.45	1.60	1.60	1.65	1.55
Cr	n.d.	n.d.	n.d.	n.d.	0.00	0.00	0.00	0.00
Ca	0.00	0.00	0.01	0.00	0.01	0.00	0.00	0.00
Fe	0.79	0.76	0.75	0.79	1.17	1.36	1.32	1.43
Mg	1.83	1.88	1.85	1.77	1.21	1.13	1.12	1.08
Mn	0.00	0.00	0.00	0.00	0.00	0.00	0.01	0.01
K	0.91	0.89	0.92	0.93	0.75	0.83	0.87	0.89
F	0.13	0.12	0.17	0.17	n.d.	n.d.	n.d.	n.d.
Cl	0.01	0.01	0.01	0.01	n.d.	n.d.	n.d.	n.d.
∑ Cat.	8.06	8.01	8.12	8.11	7.76	7.83	7.87	7.89

Table 6: Representative electron microscope analyses of selected biotites of the Glöselhof Lithodeme. Cations are calculated on the basis of 11 oxygens and 7 cations + Na + K + Ca.

as meroxene whereas biotite in muscovite dominated mica schists is discriminated mainly as lepidomelane according to Tröger (1982) (Tab. 6).

Amphibole (Tab. 7) is plotting in the tschermakite/pargasite field. Further discrimination diagrams for calcic amphiboles after Leake et al. (1997) identifies them as ferro-tschermakites. The structural cation distribution after Spear and Kimball (1984) is shown in Table 8.

According to the diagrams of Laird and Albee (1981) and Spear (1993) (Fig. 5) amphiboles of the Glöselhof Lithodeme plot in the fields of the garnet and high garnet zone, corresponding to upper greenschist facies to lower amphibolite facies conditions.

Garnet is almandine-rich within the range Alm_{62-67} Gro_{19-23} Py_{4-6} $Spess_{5-14}$ and occurs as polyphase as well as monophase porphyroblasts (Tab. 9).

Figure 6A shows a typical example in which a small, inclusion free core region is overgrown by a broad and inclusion rich zoned rim. The chemical profile shows a pronounced discontinuous distribution of the X_{Alm}, X_{Gro}, X_{Spess} values which are significantly lower (X_{Gro}) or higher (X_{Alm}, X_{Spess}) in the core. The chemical composition of the core is constant in contrast to the rim where X_{Alm} is increasing and X_{Spess} decreasing towards the margins. X_{Gro} is slightly fluctuating and X_{Pyp} remains constant with similar values as in the core.

Similar chemical zonation patterns are also observed in the garnet cluster indicated in Figure 7, even if they are more complex due to growth and cutting effects. The large garnet crystal in the centre of Figure 7A shows again a core (Grt1a) with increasing X_{Alm}, decreasing X_{Spess}, fluctuating X_{Gro} and a more or less constant X_{Pyp}. At the right side it is overgrown by a chemically different rim with higher X_{Gro} and lower X_{Spess}, whereas X_{Alm} is slightly decreasing towards the margin. Smaller garnet crystals (Grt1b, Grt1c) are bordering the large one (Grt1a) on ist upper left border. Their cores show similar compositions as the margins of Grt1a and are interpreted as crystals that started to grow when Grt1a already existing. Their rims Grt2 are similar to the rim of Grt1a. The garnet crystal in the lower left corner of Figure 7A, enlarged presented in Figure 7B, shows a core (Grt1d) with a similar composition as the margins of Grt1a and is overgrown by a very thick rim (Grt2). This zoning indicates a marginal section through a big crystal such as Grt1a.

The second type of garnet in the Glöselhof Lithodeme shows a continuous and symmetric zoning in all major elements (Fig. 6B). A general trend in composition in which X_{Alm} and X_{Gro} increase and X_{Spess} decreases is observed. The bell-shaped curve for X_{Spess} indicates a prograde monophase character.

Unit	Glöselhof Lithodeme						Rossegg C.
Rock	mica schist						amphibolite
Sample	KP-14	KP-14	KP-17	KP-17	KP-18	KP-18	KP-22
Data point	Am 1	Am 2	Am 1	Am 2	Am 1	Am 2	Am 1
SiO_2	40.77	40.45	41.52	41.73	41.07	40.95	40.63
TiO_2	0.41	0.31	0.24	0.43	0.25	0.28	0.44
Al_2O_3	18.37	17.86	18.75	18.11	18.78	17.97	16.55
Cr_2O_3	0.00	0.06	0.13	0.03	0.00	0.00	0.04
Fe_2O_3	2.14	2.65	2.21	2.24	2.84	2.91	3.18
CaO	9.66	10.06	10.10	10.19	9.98	10.12	9.63
FeO	18.90	19.20	18.36	18.88	19.53	19.72	20.49
MgO	5.11	5.56	5.66	5.70	5.17	5.31	5.31
MnO	0.12	0.20	0.21	0.23	0.00	0.21	0.26
K_2O	0.48	0.48	0.35	0.47	0.49	0.63	0.61
Na_2O	2.10	1.95	2.00	1.88	1.66	1.54	1.99
F	0.27	0.24	0.32	0.24	n.d.	n.d.	0.27
Σ [wt%]	98.33	99.02	99.85	100.13	99.77	99.64	99.40
Si	6.21	6.17	6.21	6.23	6.17	6.19	6.25
Ti	0.05	0.04	0.03	0.05	0.03	0.03	0.05
Al	3.30	3.21	3.31	3.19	3.32	3.20	3.00
Cr	0.00	0.01	0.02	0.00	0.00	0.00	0.00
Fe^{3+}	0.24	0.30	0.25	0.25	0.32	0.33	0.37
Ca	1.58	1.64	1.62	1.63	1.60	1.64	1.59
Fe^{2+}	2.13	2.11	2.02	2.08	2.10	2.12	2.22
Mg	1.16	1.26	1.26	1.27	1.16	1.19	1.22
Mn	0.02	0.03	0.03	0.03	0.00	0.03	0.03
K	0.09	0.09	0.07	0.09	0.09	0.12	0.12
Na	0.62	0.58	0.58	0.55	0.48	0.45	0.59
F	0.13	0.12	0.15	0.11	n.d.	n.d.	0.13
Σ Cat.	15.53	15.55	15.53	15.48	15.27	15.30	15.58

Table 7: Representative electron microscope analyses of selected amphiboles. Cations are calculated on the basis of 23 oxygens and 13 cations for the T- and C-position.

4.2.3 Thermometry

The metamorphic P-T conditions for the Glöselhof Lithodeme are estimated using selected cation-exchange thermometers with the software package PET 7 (Dachs, 1998). Because of missing suitable mineral parageneses all calculated temperatures are related to a pressure of 0.8 GPa which corresponds to a geothermal gradient of about 20°C/km (Schuster et al., 2004) being typical for the Austroalpine unit during Eoalpine prograde metamorphism.

The garnet-chlorite-thermometer of Perchuk (1991), applied to samples KP14, 17 and 18, yielded temperatures between 520 and 530°C (Fig. 8A). Temperature calculations using the garnet-amphibole thermometer of Dale et al. (2000) were used for samples KP14 and KP17. Calculated temperatures are almost exactly 510°C (Fig. 8A). Furthermore, the garnet-biotite-thermometer using the calibration of Holdaway (2000) was applied to sample KP16 and 17. Based on this thermometer, the temperatures were in the range from 550°C to 580°C (Fig. 8B).

4.3 Rossegg Compex (Waxenegg Nappe/ ACU)

The Rossegg Complex of the Waxenegg Nappe has recently been introduced in the map by Matura and Schuster (2014). Ist variegated successions are best exposed in the surrounding of the village Rossegg, about 35 km ENE of Graz. It also forms the north-western corner of the Radegund Crystalline Unit indicated as amphibole bearing mica schists in the map by Flügel et al. (2011). The Rossegg Complex is dominated by graphitic, hornblende bearing mica schists and carbonaceous mica schists with layers of graphite schists, amphibolites and

different types of marbles and quartzites (Schuster et al., 2014). In the ACU the schistosity is WNW to S dipping with moderate angles. A stretching lineation dips towards SW and is parallel with rotated axes of folded quartz mobilisate layers.

4.3.1 Petrography

Garnet-mica schists consist of muscovite, garnet of varying size, quartz, chlorite and chloritoid. In sample KP23 amphibole, zoisite/clinozoisite, plagioclase and epidote appear additionally. Accessories are allanite, apatite, rutile, tourmaline, zircon and opaque phases like ilmenite and pyrite. The rocks show a distinctive schistosity of the mica- and quartz-rich matrix. Chlorite appears in two different generations: (1) as primary chlorite in the matrix without any contact to garnet grains and (2) as secondary chlorite replacing garnet (Fig. 9A). Large hypidioblastic garnets, a few mm in size, occur as porphyroblasts with a syn-deformative internal texture indicative for shearing to the NE (Fig. 9B). The cores of the garnets show a poikiloblastic character and the amount of inclusions decreases towards the rims. Typical inclusions in garnet are tourmaline and light green and twinned chloritoid (Fig. 9C). No chloritoid occurs within the matrix of the mica schists from the Rossegg Complex but Krenn et al. (2008) described the appearance of staurolite from the quarry near to Steg.

White mica-rich amphibolites consist of amphibole (ferrotschermakite), muscovite, calcite, quartz, plagioclase and minor biotite and chlorite. Accessories are apatite, rutile and magnetite. Recrystallised calcite and quartz occur as folded layers (Fig. 9D).

4.3.2 Mineral chemistry

White mica have an average Si content of 6.3 a.p.f.u. and are Fe rich with 2.98 wt.% (Tab. 2).

Chlorite can be classified as chamosite according to Bailey (1988) (Tab. 3).

Chloritoid is chemically homogeneous (Tab. 4) and occur as inclusions in syn-deformative garnets (Fig. 9C).

Amphibole is classified as ferro tschermakite by using diagrams after Leake et al. (1997) (Tab. 7).

Garnet appears as monophase (Fig. 9A-C) and polyphase porphyroblasts (Fig. 9E, F). The monophase grains and the rims are almandine-rich within the range Alm_{73-80} Gro_{10-13} Py_{6-8} $Spess_{2-8}$ (Tab. 9).

4.4 Rappold Complex (Radegund Nappe/ACU)

The Rappold Complex is widespread in the eastern part of the Eastern Alps. It is dominated by dark greyish, graphitic paragneisses and mica schists with intercalations of marbles, amphibolites, quartzites and Permian pegmatites (Esterlus, 1983, 1986). Garnets in the metapelites show a distinctive polymetamorphic character. Based on Sm-Nd ages on garnet cores and U–Th–Pb chemical dating on monazite, the Rappold Complex experienced a Permian metamorphic imprint (Röggla, 2007; Gaidies et al., 2008) and an Eoalpine (Cretaceous) overprint. Calculated P-T-conditions of the Permian garnet cores from the ACU are about 580±20°C at about 0.8 GPa (Röggla, 2007; Krenn et al., 2008) and are in agreement with conditions of the Rappold Complex in the Niedere Tauern mountain range (Faryad and Hoinkes, 2003; Gaidies et al., 2006). Du-

	Sample	KP-14	KP-14	KP-17	KP-17	KP-18	KP-18	KP-22
Pos.	Data point	Am 1	Am 2	Am 1	Am 2	Am 1	Am 2	Am 1
A	Na	0.30	0.34	0.31	0.28	0.18	0.18	0.32
	K	0.09	0.09	0.07	0.09	0.09	0.12	0.12
B	Ca	1.58	1.64	1.62	1.63	1.60	1.64	1.59
	Na	0.32	0.24	0.27	0.27	0.30	0.27	0.27
	Fe^{2+}	0.11	0.12	0.11	0.10	0.09	0.09	0.14
	Mn	0.00	0.00	0.00	0.00	0.00	0.00	0.00
	Mg	0.00	0.00	0.00	0.00	0.00	0.00	0.00
C	Mg	1.16	1.26	1.26	1.27	1.16	1.19	1.22
	Fe^{2+}	2.03	1.99	1.91	1.98	2.00	2.03	2.08
	Mn	0.02	0.03	0.03	0.03	0.00	0.03	0.03
	Fe^{3+}	0.24	0.30	0.25	0.25	0.32	0.33	0.37
	Al	1.51	1.37	1.52	1.42	1.49	1.39	1.24
	Cr	0.00	0.01	0.02	0.00	0.00	0.00	0.00
	Ti	0.05	0.04	0.03	0.05	0.03	0.03	0.05
T	Si	6.21	6.17	6.21	6.23	6.17	6.19	6.25
	Al	1.79	1.83	1.79	1.77	1.83	1.81	1.75
OH	OH	1.87	1.88	1.85	1.89	2.00	2.00	1.87
	F	0.13	0.12	0.15	0.11	0.00	0.00	0.13

Table 8: The structural distribution of cations after Spear and Kimball (1984) for the same amphibole analyses (given in Tab. 7).

Unit	Glöselhof Lithodeme					Rossegg C.		Rapp. C.
Rock	mica schist					Grt-mica schist		
Sample	KP-14	KP-14	KP-17	KP-17	KP-17	KP-19	KP-19	KP-24
Data point	Grt 1	Grt 2	Grt 1	Grt 2	Grt 3	Grt 1	Grt 2	Grt 1
SiO_2	36.90	38.13	37.72	37.84	37.89	37.06	37.19	36.95
TiO_2	0.12	0.10	0.13	0.11	0.07	0.00	0.06	0.08
Al_2O_3	20.76	20.86	20.43	20.78	20.97	20.46	20.30	20.90
Cr_2O_3	0.03	0.00	0.00	0.03	0.03	0.00	0.09	0.00
CaO	7.56	7.74	7.47	6.59	8.04	4.43	3.72	2.93
FeO	27.97	29.64	27.90	27.69	28.62	32.13	35.48	36.48
MgO	1.08	1.49	1.33	1.17	1.45	1.49	1.97	1.93
MnO	4.53	2.19	4.71	6.30	3.33	3.51	0.64	1.32
∑ [wt%]	98.95	100.15	99.69	100.51	100.40	99.08	99.45	100.59
Si	3.00	3.05	3.04	3.04	3.02	3.03	3.03	2.97
Ti	0.01	0.01	0.01	0.01	0.00	0.00	0.00	0.00
Al	1.99	1.97	1.94	1.96	1.97	1.97	1.95	1.98
Cr	0.00	0.00	0.00	0.00	0.00	0.00	0.01	0.00
Ca	0.66	0.66	0.65	0.57	0.69	0.39	0.32	0.25
Fe	1.90	1.98	1.88	1.86	1.91	2.19	2.41	2.47
Mg	0.13	0.18	0.16	0.14	0.17	0.18	0.24	0.23
Mn	0.31	0.15	0.32	0.43	0.23	0.24	0.04	0.09
∑ Cat.	8.00	8.00	8.00	8.00	8.00	8.00	8.00	8.00
X_{Gro}	0.22	0.22	0.21	0.19	0.23	0.13	0.10	0.05
X_{Alm}	0.63	0.67	0.63	0.62	0.64	0.73	0.80	0.81
X_{Pyp}	0.04	0.06	0.05	0.05	0.06	0.06	0.08	0.08
X_{Spess}	0.10	0.05	0.11	0.14	0.08	0.08	0.02	0.03

Table 9: Representative electron microscope analyses of selected garnets of the Glöselhof Lithodeme, Rossegg Complex and Rappold Complex. Cations are calculated on the basis of 12 oxygens and 8 cations.

Sample		Rb [ppm]	Sr [ppm]	$^{87}Rb/^{86}Sr$	$^{87}Sr/^{86}Sr$ ± 2σ m
Schöckel Formation					
11R15	WR	48.34	110.8	1.2638	0.713166 ± 5
11R15	Ms	349.7	56.32	18.031	0.741020 ± 4
Raasberg Formation					
08R11	WR	81.04	229.6	1.0217	0.711384 ± 3
08R11	Bt	132.2	3.616	107.64	0.881963 ± 9
Rossegg Complex					
08R59	WR	118.2	457.1	0.7491	0.713656 ± 4
08R59	Bt	459.1	28.77	46.425	0.763481 ± 4
Rappold Complex					
05R09	WR	140.5	111.8	3.6419	0.726263 ± 4
05R09	Bt	514.1	6.743	226.43	0.975423 ± 5

Table 10: Rb-Sr data from samples of the Graz Paleozoic, Anger Crystalline Unit and Radegund Crystalline Unit.

ring the Eoalpine imprint in the Late Cretaceous amphibolite facies conditions were reached (Röggla, 2007).

In the study area, the schistosity in the Rappold Complex dips towards WSW. Stretching lineation and rotated axes of folded quartz mobilisate layers plunge to the SW with shallow to moderate angles (Schuster et al., 2014).

4.4.1 Petrography

The mineral assemblage of the garnet-mica schists from the Rappold Complex is composed of muscovite, quartz, garnet, plagioclase and biotite. Garnet mostly occurs as polyphase porphyroblasts with large cores and irregular rims formed by tiny crystals. In the cores inclusions of biotite, plagioclase or chloritoid occur (Röggla, 2007; Gaidies et al., 2006). Staurolite has been described by Schaflechner (2002), Röggla (2007) and Krenn et al. (2008). As accessories allanite, rutile, tourmaline and zircon occur. No chloritoid is observed in the matrix, but is present as inclusions within garnet porphyroblasts (Fig. 9G). The mm-sized garnets show poikiloblastic textures and are in some samples completely altered and replaced by chlorite and quartz. A second type of garnet which is more homogeneous with a lower amount of inclusions is also observed. Plagioclase occurs in a foliated quartz-mica-rich matrix and shows a poikiloblastic texture (Fig. 9H).

4.4.2 Mineral chemistry

White mica has an average Si content of 6.28 a.p.f.u. and moderate FeO content of 1.55 wt.% (Tab. 2).

Chlorite is determined as chamosite according to Bailey (1988) (Tab. 3).

Chloritoid is characterised by an average FeO content of 24.61 wt.%, a MgO content of 2.24 wt.% and a MnO content of 0.15 wt.% (Tab. 4).

Garnet core composition show an average mole fraction of X_{Gro} 0.05, X_{Alm} 0.81, X_{Pyp} 0.08 and X_{Spess} 0.03 (Tab. 9).

4.5 Geochronology

Analytical results for the Rb-Sr mica ages are shown in Figure 11 and Table 10.

From the Schöckel Nappe a biotite bearing calcareous schist from the Raasberg Formation near to Anger (08R11) and an impure marble with muscovite from the Schöckel Formation north of Ponigl (11R15) was dated. The biotite age is 112.6 ± 1.1 Ma whereas the muscovite yielded 119.2 ± 1.2 Ma.

Two samples (08R56, 05R09) were collected from the complexes of the Koralpe-Wölz Nappe System. A mica schist with biotite prophyroblasts from the Rossegg Complex near to the village of Rossegg shows an Rb-Sr biotite age of 76.8 ± 0.8 Ma. From the Rappold Complex of the Radegund Crystalline Unit a kyanite bearing gneiss was dated with an Rb-Sr biotite age of 78.7 ± 0.8 Ma.

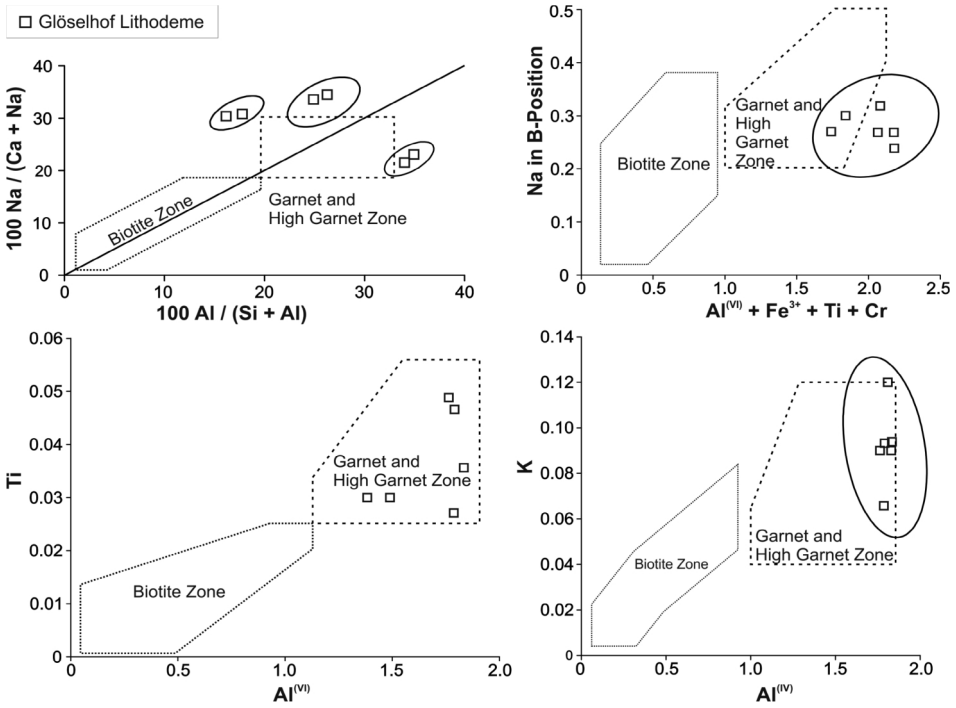

Figure 5: Amphibole plots of the Glöselhof Lithodeme based on 23 cations per oxygens for estimating P-T-conditions according to Spear (1993). Diagrams implicate upper greenschist-/amphibolite facies conditions.

5. Discussion

In the following chapter data from the Glöselhof Lithodeme, Hirschkogel Lithodeme, Rossegg Complex and Rappold Complex are summarised and compared with each other. Important parameters are the presence of index minerals, P-T data and geochronological data from the literature. In general the units are discussed from top to the bottom.

5.1 Occurrence of chloritoid and other index minerals in metapelites

In the fine-grained mica schists of the Glöselhof Lithodeme at the base of the Gschnaidt Nappe white mica, biotite, garnet and amphibole are present. Garnet zoning indicates a polyphase metamorphic history. Phyllites of the Schöckel Nappe are characterised by mineral assemblages including white mica, chlorite and chloritoid. Chloritoid is present in several lithostratigraphic units (Flügel and Maurin, 1958) but it is most frequent in the Hirschkogel Lithodeme. Up to 2 cm large chloritoid porphyroblasts occur within pelites of the Raasberg Formation. They appear together with tiny staurolite crystals within a matrix of fine-grained white mica (Schuster et al., 2014) (Fig. 10).

In the Rossegg Complex of the ACU medium-grained mica schists with biotite, garnet and amphibole are typical. Garnet appears as polyphase and monophase crystals and chloritoid is present as inclusions only within the rims of polyphase garnets and within monophase garnet crystals. Metapelites in the Rappold Complex are represented by medium-grained mica schists and paragneisses, containing biotite, garnet and staurolite. Garnet shows a polyphase evolution. In mica schists chloritoid appears in the cores of the garnets. These cores are in equilibrium with relics of staurolite in the rock matrix (Röggla, 2007). In paragneisses the garnet cores are characterised by inclusions of biotite and plagioclase.

Zoning of the index minerals has already been described in Neubauer (1982) and Krenn et al. (2008). However, tectonic subdivision based on the map by Matura and Schuster (2014) indicates a less continuous zonation than previously thought. For revealing continuous or discontinuous metamorphic successions it is critical to compare index minerals formed during the same metamorphic event. For this reason the timing of the metamorphic imprints in the individual units has to be considered.

5.2. Polymetamorphism and age of metamorphism

Based on garnet textures and chemical profiles (Figs. 3, 6, 7, 9) a polymetamorphic evolution is indicated for the Glöselhof Lithodeme as well as for the Rossegg and Rappold complexes. The garnets in the individual units are different in size, they contain different types of inclusions and differences in their matrix, but they show similarities in their chemical zoning. In general X_{Gro} in the cores is lower and increases towards the rim. For the Rappold Complex the formation age of the garnet cores is known, whereas for all other units the garnet age has to be estimated indirectly, e.g. from cooling ages or structural data.

According to the own observations and literature data (Schuster et al., 2004; Röggla, 2007) the units of the ACU experienced an epidote amphibolite or amphibolite facies Eoalpine (Cretaceous) metamorphic imprint with contemporaneous growth of garnet. During this imprint the monophase garnets and the garnet rims with inclusions of chloritoid in the Rossegg Complex as well as the garnet rims in the Rappold Complex developed. The garnets are correlated to ductile deformation cau-

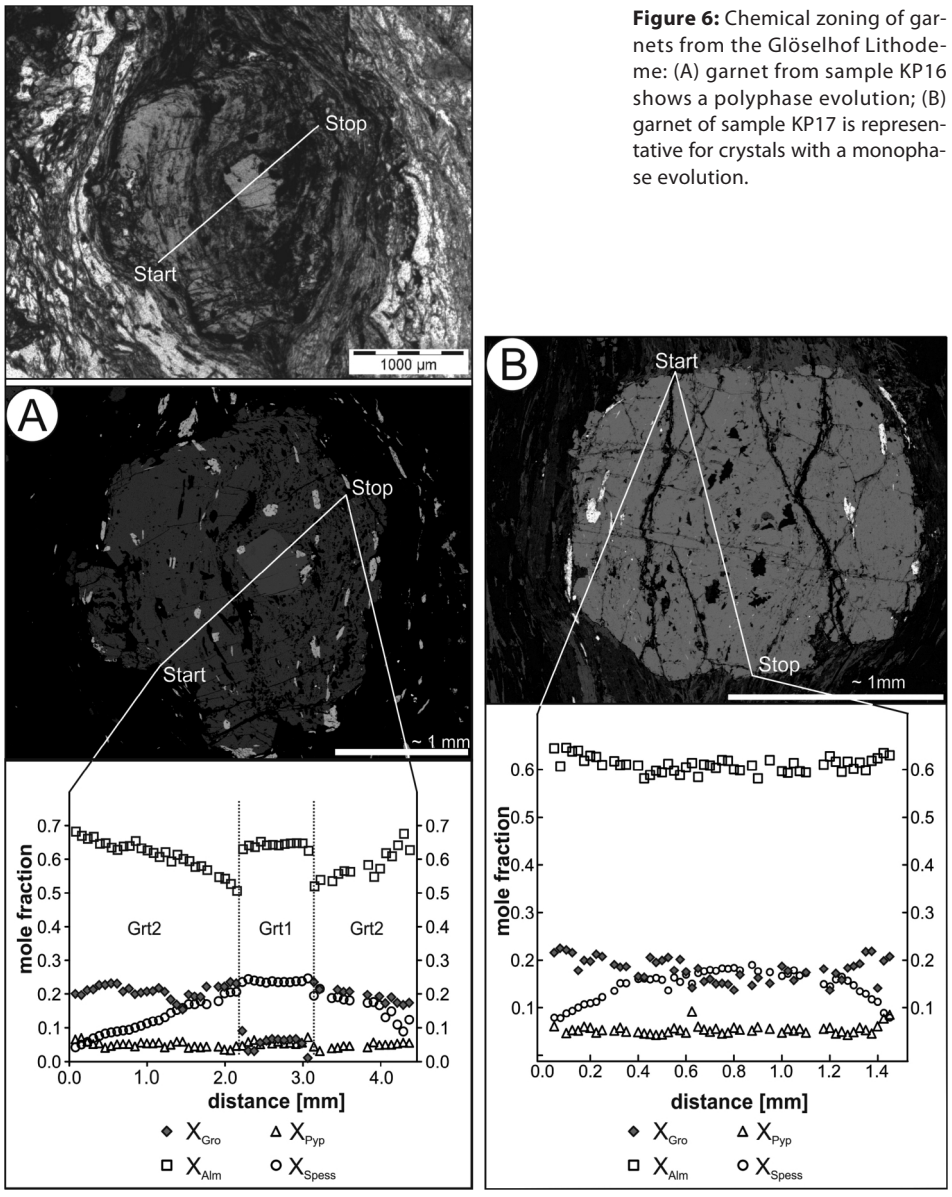

Figure 6: Chemical zoning of garnets from the Glöselhof Lithodeme: (A) garnet from sample KP16 shows a polyphase evolution; (B) garnet of sample KP17 is representative for crystals with a monophase evolution.

sing a mostly SW dipping schistosity, SW dipping stretching lineations and ductile fold axes. Locally, younger fold axes are NW-SE orientated (Schantl and Brandner, 2013). According to Thöni (2006) the peak of the Eoalpine imprint in the Koralpe-Wölz-Nappe System occurred in the Turonian at about 92 Ma. Typical Rb-Sr biotite ages from several complexes of the ACU are about 80 Ma (Fig. 11). They are interpreted to reflect cooling below 300 ± 50°C (Jäger et al., 1967).

The contact of the ACU to the overlying GP is a ductile shear zone and the structures in the GP show similar orientations (Krenn et al., 2008; Schantl and Brandner, 2013; Schuster et al., 2014). Therefore the second metamorphic event in the Glöselhof Lithodeme of the Gschnaidt Nappe and the metamorphic imprint in the Schöckel Nappe are Cretaceous in age. This is supported by the Rb-Sr mica ages of muscovite in the impure marble which formed at 119.2 ± 1.2 Ma. Since the Schöckel Nappe is characterised by greenschist facies conditions, which is lower or in the range of the closure temperature of the Rb-Sr isotopic system in muscovite (550 ± 50°C, Purdy and Jäger, 1976), this age is interpreted to date muscovite formation close to the metamorphic peak. The Rb-Sr biotite age of 112.6 ± 1.1 Ma from the biotite bearing carbonaceous schist reflects cooling below c. 300°C, in the Early Cretaceous.

Based on the presented geochronological data and data from the literature (see summary in Gasser et al., 2010) a metamorphic imprint in the Early Cretaceous, contemporaneous to the formation of ductile structures in the lower nappe group of the GP is concluded. This interpretation is in line with Fritz et al. (1992).

Schuster et al. (2004) postulated in the eastern part of the Koralpe-Wölz Nappe System a Permian high temperature/low pressure metamorphic imprint predating the Cretaceous one. During the Permian imprint the garnet cores in the Rappold Complex (Röggla, 2007; Gaidies et al., 2008), overgrowing chloritoid, biotite and plagioclase formed in assemblage with staurolite (Röggla, 2007). Contemporaneously the pegmatites in the Rappold Complex intruded. Also the garnet cores in the underlying Wölz Complex are Permian in age (Schuster et al., 2001; Röggla, 2007) and therefore development of the garnet cores in the Rossegg Complex during the Permian event is likely.

For the GP polyphase mineral assemblages are described for the first time here. The cores of polyphase garnets from the Glöselhof Lithodeme are small (< 0.5 mm; Fig. 6A and 7) and not suitable for Sm-Nd dating. Partly they show complex chemical zonings but in general the cores are characterised by lower X_{Gro} with respect to the rims. This is similar to garnets with Permian cores and Cretaceous rims from other units (e.g. Wölz and Rappold complexes), and might indicate a Permian metamorphic imprint in the Glöselhof Lithodeme, too. However, also Variscan garnet cores of the Austroalpine Unit show this feature, e.g. garnets of the Bundschuh Complex (Koroknai et al., 1999; Schuster and Frank, 1999). Fur-

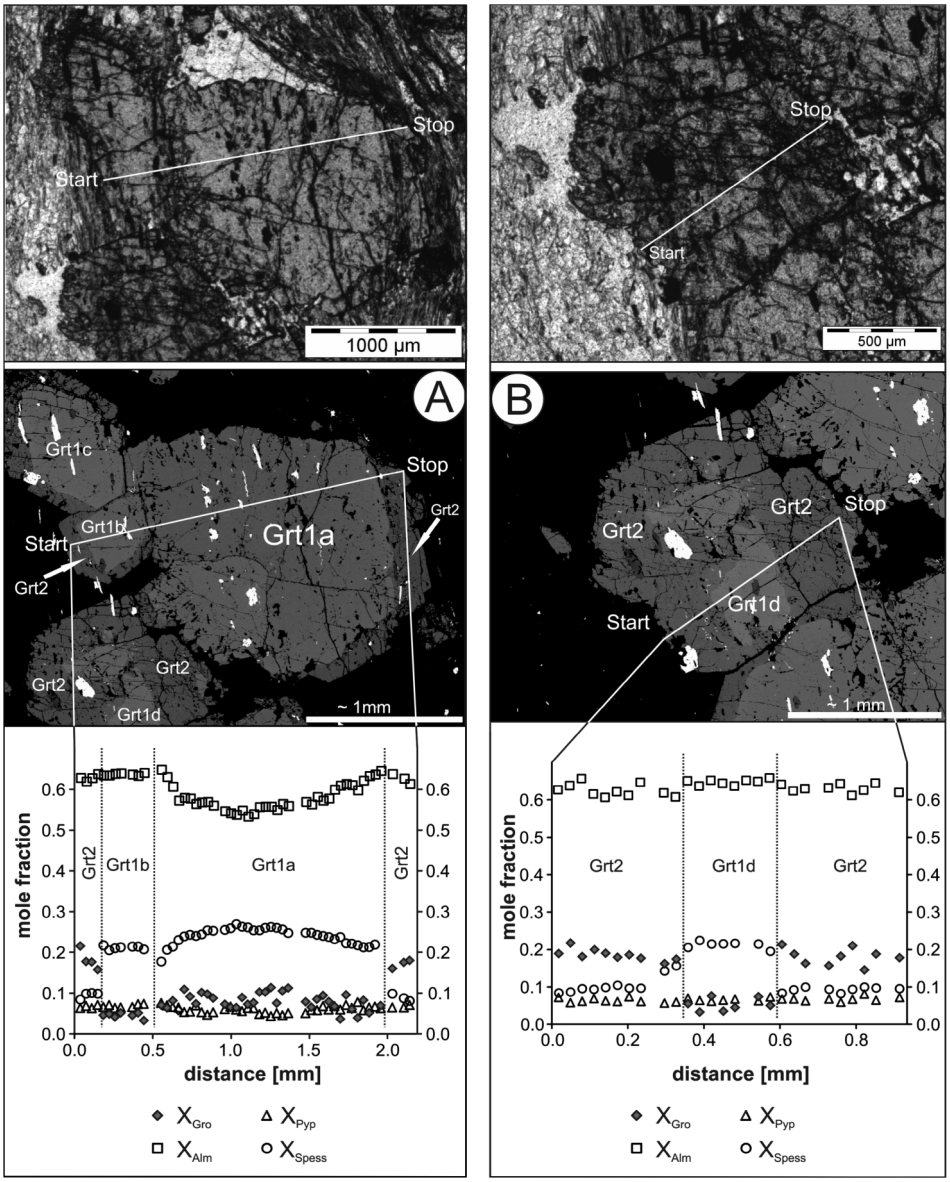

Figure 7: Chemical zoning of garnets from the Glöselhof Lithodeme: garnet cluster with crystals showing a polyphase evolution (sample KP17). Slight differences of the individual grains are due to different time of nucleation and cutting effects; (A) overview picture; (B) detail.

ther a Variscan metamorphic imprint has been proposed for other units of the GP (Neubauer et al., 1999). In conclusion, the age of the first metamorphic imprint in the Glöselhof Lithodeme will have occurred during the Variscan or Permian event.

5.3 Eoalpine P-T conditions within the study area

Eoalpine temperatures for the Glöselhof Lithodeme (Gschnaidt Nappe/GP), calculated with the garnet-chlorite and garnet amphibole thermometer, range between 510-530°C for an assumed pressure of 0.8 GPa. This value indicates epidote-amphibolite facies peak conditions, which is in good agreement with the macroscopic and microscopic behaviour of the fine-grained garnet bearing mica schists. Temperatures calculated by garnet-biotite thermometry yield somewhat higher temperatures of 550-580°C indicative for lower amphibolite facies conditions. Muscovites from the Glöselhof Lithodeme reveal the highest average phengite contents (3.26 Si a.p.f.u.) of all investigated units (Fig. 12).

In comparison to other investigated units, muscovites of the Hirschkogel Lithodeme (Schöckel Nappe/GP) reflect the lowest phengite contents with an average value of 3.07 Si a.p.f.u., indicative for relative low pressure conditions assuming a similar bulk rock composition (Fig. 12). Based on the mineral chemical data and the fact that garnet is missing, lower greenschist facies conditions with temperatures of less than 500°C can be expected.

Metamorphic conditions in the Rossegg Complex (ACU) were somewhat higher than in the Glöselhof and Hirschkogel lithodemes, based on coarser-grain size and on the occurrence of garnet together with staurolite. With respect to Krenn et al. (2008) amphibolite facies conditions of 580 ± 10°C at about 0.8 GPa are assumed. For the Rappold Complex (ACU) somewhat higher amphibolite facies conditions of 630 ± 10°C and 0.94 ± 0.01 GPa have been determined by Röggla (2007).

5.4 Metamorphic zoning of the Eoalpine metamorphic event and its implications for the relation of the GP and ACU

Based on the distribution of index minerals and the P-T data the following metamorphic zoning for the Eoalpine metamorphic event can be summarised (Fig. 13B). In general there is a temperature decrease from the GP towards the ACU. Within the investigated area of the GP a tectonically inverted metamorphic field gradient has been determined in the study area. The uppermost Gschnaidt Nappe shows epidote-amphibolite facies conditions with temperatures of more than 510°C. Less than 500°C have been estimated for the underlying Schöckel Nappe and according to Schuster et al. (2014) even lower temperatures are expected for the lowermost Gasen Nappe. The directly underlying Rossegg and Rappold complexes of the ACU are characterised by amphibolite facies conditions and an upright metamorphic field gradient. These observations argue against tectonic thinning of a continuous section from the GP into the ACU during Eoalpine post peak metamorphic normal faulting.

Also the geochronological age data support a complex history (Fig. 13C). In the GP nappe stacking, heating and subsequent cooling occurred in the Early Cretaceous (> 100 Ma). In contrast in the ACU the metamorphic peak assemblages have been established in the Late Cretaceous (Turonian) and subsequent exhumation of the deeply buried rocks formed the Koralpe-Wölz Nappe System by ductile thrusting and normal faulting. Cooling in the ACU below the ductile/brittle transition (c. 300°C) occurred in the Campanian at ca. 80 Ma.

The inverted metamorphic field gradient in the GP in contrast to the upright field gradient in the investigated part of the ACU as well as the different thermal evolutions indicate a major thrust in between these two units. In the study area the boundary is represented by a steeply dipping thrust, but

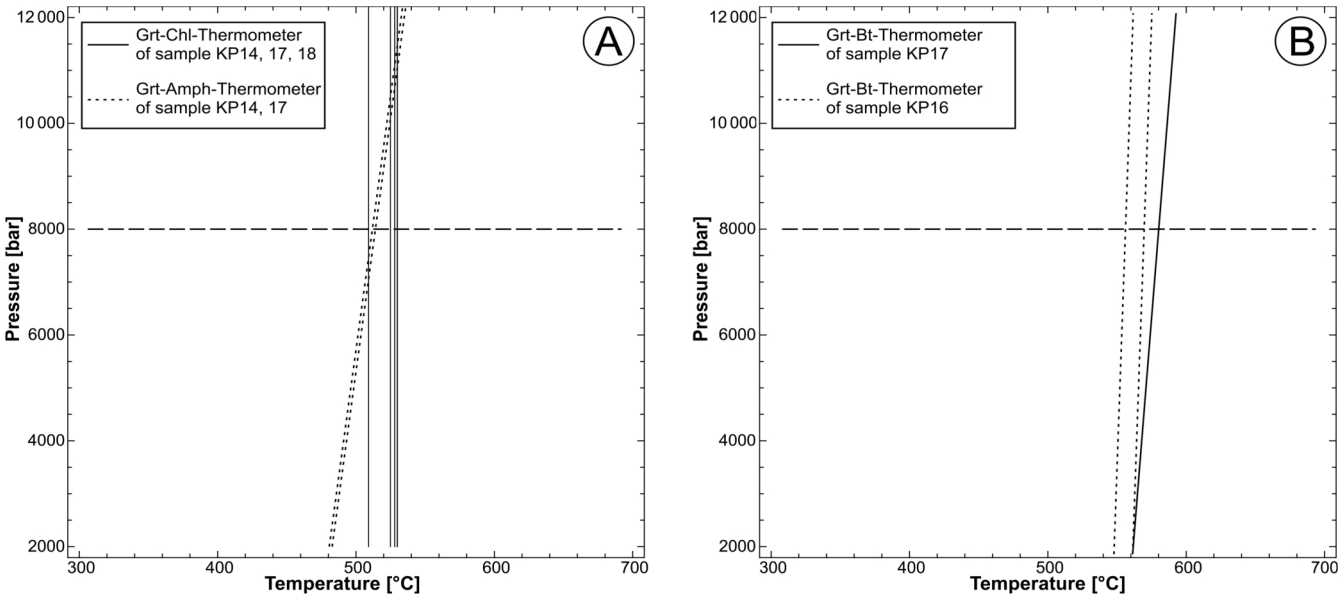

Figure 8: Calculated temperatures of the Glöselhof Lithodeme: (A) garnet-chlorite-thermometry (continuous line) and garnet-amphibole thermometry (dotted line); (B) garnet-biotite-thermometry of sample KP17 (continuous line) and sample KP16 (dotted line).

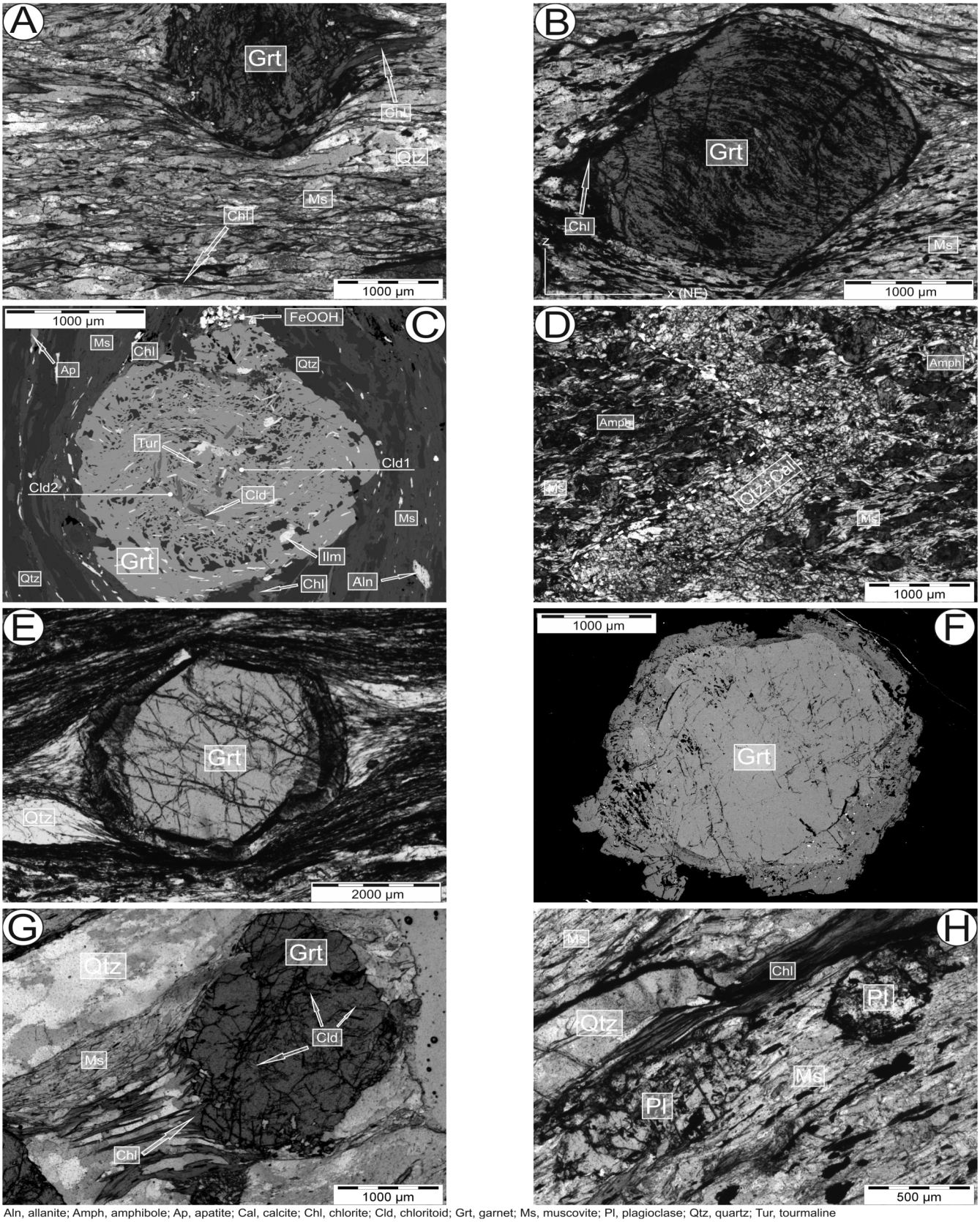

Aln, allanite; Amph, amphibole; Ap, apatite; Cal, calcite; Chl, chlorite; Cld, chloritoid; Grt, garnet; Ms, muscovite; Pl, plagioclase; Qtz, quartz; Tur, tourmaline

Figure 9: Petrography of metapelites and metabasites from the Rossegg Complex and Rappold Complex: (A) syn-deformative garnet from the Rossegg Complex retrogressed and replaced by syn-deformative secondary chlorite; primary chlorite occurs within the matrix; (B) syndeformative garnet from the Rossegg Complex with intern foliation indicative for shearing to the SW; (C) BSE-image indicating the occurrence of chloritoid-inclusions in garnet within the Rossegg and Rappold complexes and analysed chloritoids of the Rossegg Complex are numbered and indicated in Table 4; (D) amphibolite containing a folded quartz-calcite layer and shows an axial plane cleavage; (E) view of thin section with a polyphase garnet from the Rossegg Complex (sample 08R56, width 7 mm); (F) BSE image of a polyphase garnet from the Rossegg Complex (sample 08R56); (G) garnet from the Rappold Complex with inclusions of chloritoid and chlorite growth in pressure shadows of the garnet grain; (H) plagioclase blasts within a matrix consisting of quartz, muscovite and chlorite (Rappold Complex).

with respect to the map by Matura and Schuster (2014) there is a phyllonite zone in between the Wölz Complex (ACU) and the Gasen Nappe, which forms the lowermost nappe of the GP at its eastern margin. This phyllonite zone formed at lower greenschist facies conditions and has to be Late Cretaceous in age as the Rb-Sr biotite ages in the ACU are about 80 Ma. This is in agreement with conclusions after Krenn et. al. (2008).

6. Conclusions

Petrological investigations based on the map by Matura and

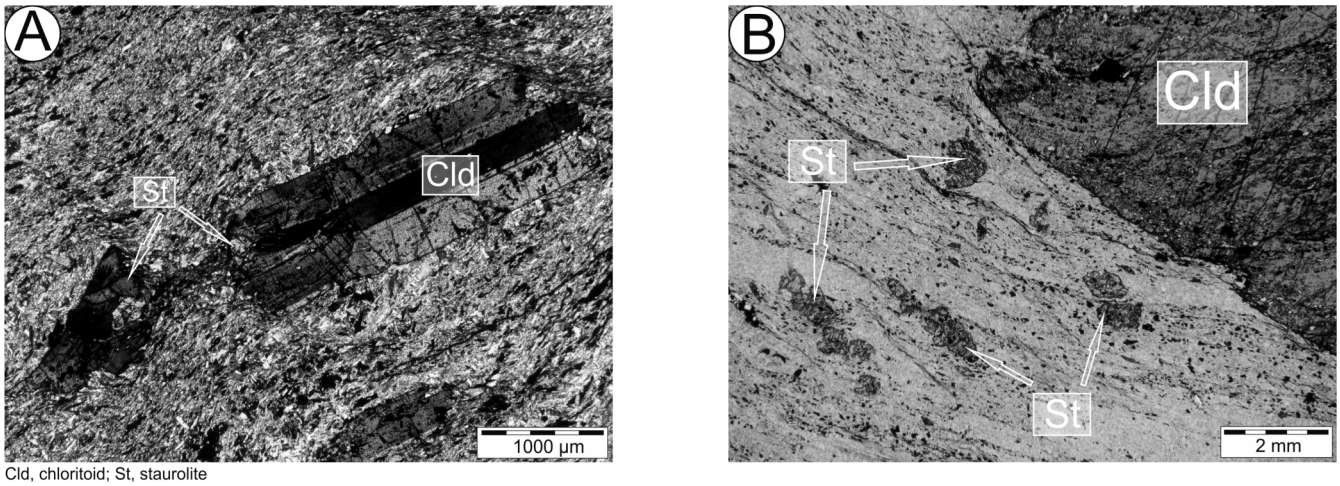

Cld, chloritoid; St, staurolite

Figure 10: Chloritoid porphyroblasts (up to 2cm in size) appear together with tiny staurolite within pelites from the Raasberg Fomation (A and B).

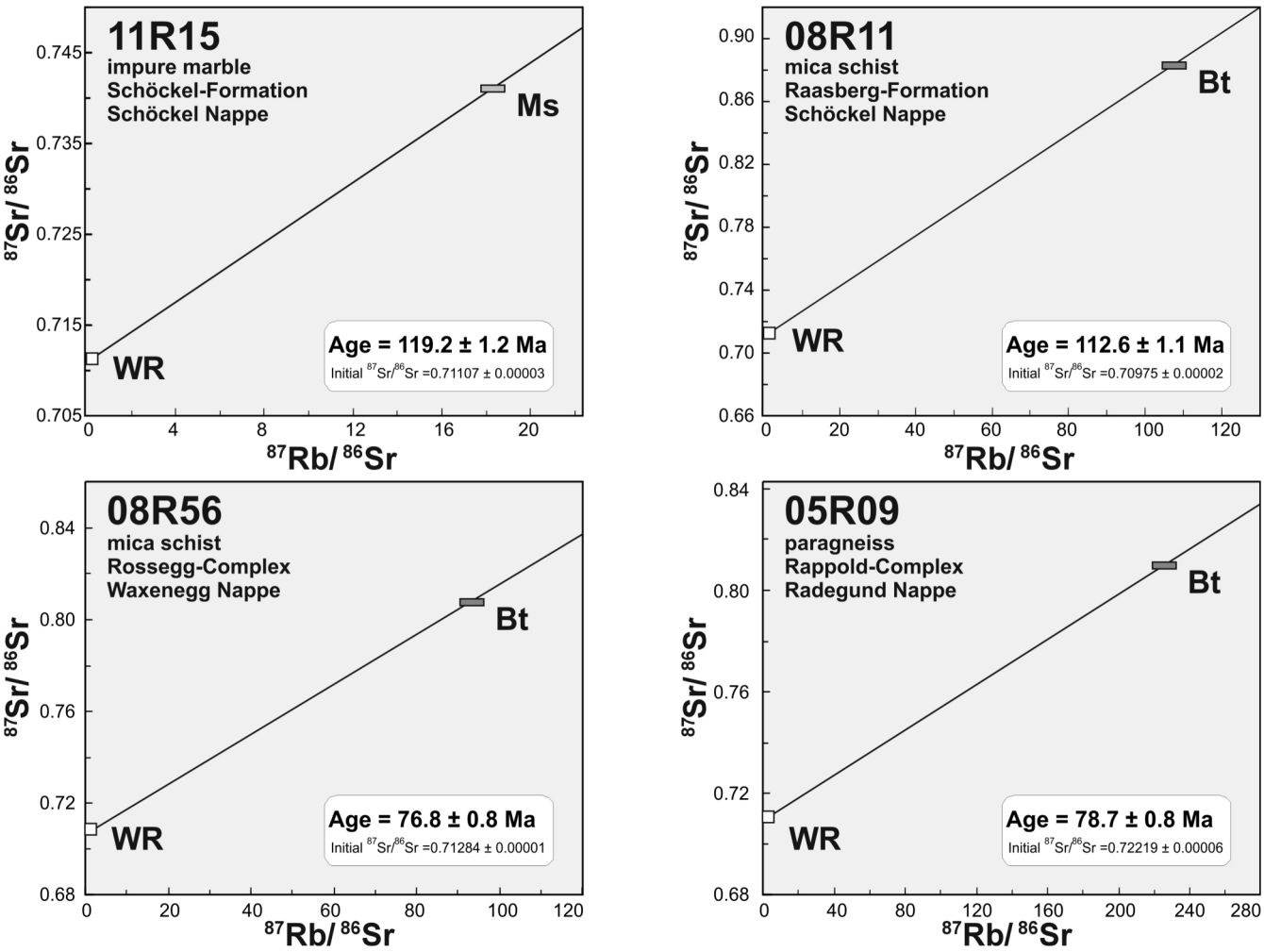

Figure 11: Rb-Sr diagrams for micas from the Graz Paleozoic, Anger Crystalline Unit and Radegund Crystalline Unit. The ages from the GP indicate an Early Cretaceous metamorphic imprint, whereas cooling in the ACU and RCU occurred in the Late Cretaceous (for explanation see text).

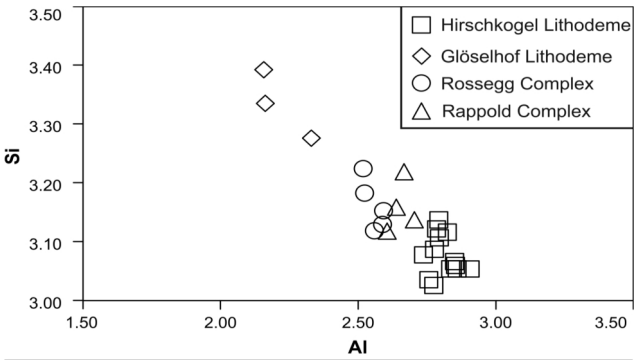

Diagram shows muscovites of Table 2 and additional selected analyses.

Figure 12: Si vs. Al plot of analysed muscovites show the linear exchange between these two cations according to the Tschermak substitution. Muscovites of the Hirschkogel and Glöselhof lithodemes show the lowest and the highest phengite contents, respectively.

Schuster (2014) revealed the following conclusions for the southeastern area of the Graz Paleozoic and the underlying complexes of the Anger Crystalline Unit:

- Index minerals exhibit a complex metamorphic zoning and garnets indicate a complex metamorphic pattern and a polymetamorphic evolution for the Glöselhof Lithodeme, Rossegg Complex and Rappold Complex (see also Röggla, 2007).
- Based on petrologic observation in combination with geochronological and structural data the whole nappe pile is dominated by an Eoalpine (Cretaceous) metamorphic imprint. The previous imprint in the complexes of the ACU is Permian in age, whereas in the Glöselhof Lithodeme of the GP it may be related to the Variscan or Permian event.
- Within the GP of the study area the Eoalpine event shows an inverted metamorphic field gradient. Epidote-amphibolite facies conditions and temperatures of more than 510°C in the Gschnaidt Nappe with, less than 500°C in the underlying Schöckel Nappe and even lower temperatures in the lowermost Gasen Nappe are proposed. In contrast, in the ACU an upright Eoalpine metamorphic zoning is established.
- The different metamorphic pattern and the time constraints indicate a major Eoalpine thrust between the GP and ACU which developed under green-schist facies conditions in the Late Cretaceous.

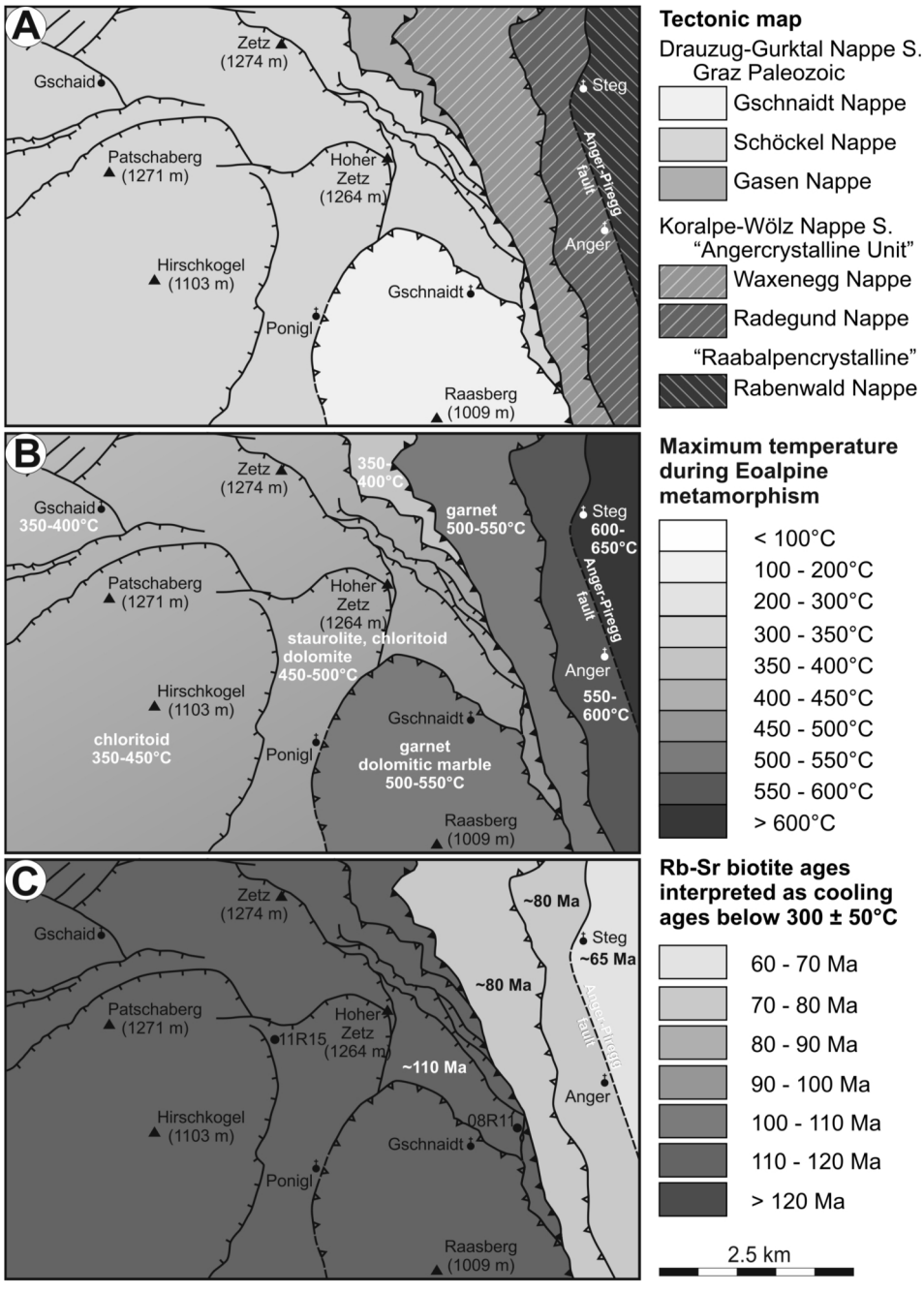

Figure 13: Summary of data presented in this study: (A) tectonic overview map of the investigated area based on Matura and Schuster (2014); (B) map showing the metamorphic zoning, including additional data from Tropper et al. (2001), Röggla (2007) and Schantl and Brandner (2013); (C) map showing the distribution of the regional cooling below ~300 °C, based on Rb-Sr biotite ages, including data by Scharbert (1990).

Acknowledgements

We thank Jürgen Neubauer and Peter Onuk for their help with electron microscope analyses. Christoph Hauzenberger is thanked for his help in calculating mineral chemical and geothermometric results. Many thanks also to Stanislaw Grabala

(Geological Survey of Austria) for mechanical sample preparation and Monika Horschinegg (University of Vienna) for her help with the isotopic analyses. We also thank a lot Franz Neubauer and Gert Rantitsch for their detailed reviews to improve the manuscript, and Michael Wagreich is thanked for his careful editorial work.

References

Bailey, S.W., 1988. Chlorites: Structures and crystal chemistry. In: S.W. Bailey (ed.) Hydrous Phyllosilicates (Exclusive of Micas). Mineralogical Society of America, Reviews in Mineralogy, 19, 347-403.

Dachs, E., 1998. PET: Petrological elementary tools for Mathematica. Computers & Geosciences, 24, 219-235. http://dx.doi.org/10.1016/S0098-3004(97)00141-6

Dale, J., Holland, T., and Powell, R., 2000. Hornblende-garnet-plagioclase thermobarometry: a natural assemblage calibration of the thermodynamic of hornblende. Contributions to Mineralogy and Petrology, 140, 353–362. http://dx.doi.org/10.1007/s004100000187

Ebner, F. and Rantitsch, G., 2000. Das Gosaubecken von Kainach - ein Überblick. Mitteilungen der Gesellschaft der Geologie und Bergbaustudenten Österreichs, 44, 157-172.

Esterlus, M., 1983. Kurzer Überblick über die Pegmatite im Angerkristallin der Oststeiermark. Archiv für Lagerstättenforschung der Geologischen Bundesanstalt, 3, 31-34.

Esterlus, M., 1986. Kristallisationsgeschichte und Strukturprägung im Kristallin des Grazer Paläozoikums. PhD thesis, University of Vienna, Vienna, 187 pp.

Faryad, S.W. and Hoinkes, G., 2003. P-T gradient of Eo-Alpine metamorphism within the Austroalpine basement units east of the Tauern Window (Austria). Mineralogy and Petrology, 77, 129–159. http://dx.doi.org/10.1007/s00710-002-0196-1

Flügel, H.W. and Maurin, V., 1958. Geologische Karte des Weizer Berglandes 1:25.000. Verlag der Geologischen Bundesanstalt, Wien.

Flügel, H.W., 1961. Die Geologie des Grazer Berglandes: Erläuterungen zur Geologischen Wanderkarte des Grazer Berglandes 1:100.000. Mitteilungen des Museums für Bergbau, Geologie und Technik am Landesmuseum Joanneum Graz, 23, 212 pp.

Flügel, H.W., 1975. Erläuterungen zur Geologischen Wanderkarte des Grazer Berglandes 1:100.000. 2. Auflage, Mitteilungen der Abteilung Geologie, Paläontologie, Bergbau des Landesmuseums Joanneum, Sonderheft 1, 288 pp.

Flügel, H., Mauritsch, H., Heinz, H. and Frank, W., 1980. Paläomagnetische und radiometrische Daten aus dem Grazer Paläozoikum. Mitteilungen der Österreichischen Geologischen Gesellschaft, 71/72, 201–211.

Flügel, H.W. and Neubauer, F., 1984. Erläuterungen zur geologischen Karte der Steiermark. Verlag der Geologischen Bundesanstalt, Wien, 127 pp.

Flügel, H.W., Hötzel, H. and Neubauer, F., 1990. Geologische Karte der Republik Österreich 1:50000, Blatt 134 Passail. Verlag der Geologischen Bundesanstalt, Wien.

Flügel, H.W. and Hubmann, B., 2000. Die lithostratigraphische Gliederung des Paläozoikums von Graz (Österreich). Österreichische Akademie der Wissenschaften/Schriftenreihe der Erdwissenschaftlichen Kommissionen, 13, 7-59.

Flügel, H.W., Nowotny, A. and Gross, M., 2011. Geologische Karte der Republik Österreich 1:50000, Blatt 164 Graz. Verlag der Geologischen Bundesanstalt, Wien.

Frank, W., 1981. Geochronologische Datierung frühalpiner Metamorphosevorgänge in den Ostalpen (Jahresbericht 1980 des Geochronologischen Labors). Die frühalpine Geschichte der Ostalpen Jahresbericht, Montanuniversität Leoben, 2, 9-43.

Fritz, H., 1988. Kinematics and geochronology of Early Cretaceous thrusting in the northwestern Paleozoic of Graz (Eastern Alps). Geodinamica Acta, 2, 53-62. http://dx.doi.org/10.1080/09853111.1988.11105156

Fritz, H. and Neubauer, F., 1988. Geodynamic aspects of the Silurian and Early Devonian Sedimentation in the Paleozoic of Graz (Eastern Alps). Schweizer Mineralogische Petrographische Mitteilungen, 68, 359-367.

Fritz, H., Ebner, F. and Neubauer, F., 1992. The Graz thrust complex (Paleozoic of Graz). Alpaca field guide, Karl-Franzens-Universität Graz, 83–92.

Gaidies, F., Abart, R., DeCapitani, C., Schuster, R., Connolly, J.A. D. and Reusser, E., 2006. Characterisation of polymetamorphism in the Austroalpine basement east of the Tauern Window using garnet isopleth thermobarometry. Journal of Metamorphic Geology, 24, 451-475. http://dx.doi.org/10.1111/j.1525-1314.2006.00648.x

Gaidies, F., Krenn, E., de Capitani, D. and Abart, R., 2008. Coupling forward modelling of garnet growth with monazite geochronology: an application to the Rappold Complex (Austroalpine crystalline basement). Journal of metamorphic Geology, 26, 775-793. http://dx.doi.org/10.1111/j.1525-1314.2008.00787.x

Gasser, D., Stüwe, K. and Fritz, H., 2010. Internal structural geometry of the Paleozoic of Graz. International Journal of Earth Sciences, 99, 1067-1081. http://dx.doi.org/10.1007/s00531-009-0446-0

Gräf, W., 1975. Ablagerungen der Gosau von Kainach. In: H.W. Flügel (ed.) Erläuterungen zur Geologischen Wanderkarte des Grazer Berglandes 1:100.000. 2. Auflage, Mitteilungen der Abteilung Geologie, Paläontologie, Bergbau des Landesmuseums Joanneum, Sonderheft 1, 83-102.

Gross, M., Fritz, I., Piller, W.E., Soliman, A., Harzhauser, M., Hubmann, B., Moser, B., Scholger, R., Suttner, T.J. and Bojar, B.-P., 2007. The Neogene of the Styrian Basin - Guide to Excursions (Das Neogen des Steirischen Beckens - Exkursionsführer). Joannea Geologie und Paläontologie, 9, 117-193.

Hasenhüttl, C., 1994. Eine Wärmegeschichte des Grazer Berglandes. Inkohlung, Illitkristallinität, Tonmineralogie und Conodont Color Alteration Index im nördlichen Teil des Grazer Deckenkomplex. PhD thesis, Karl-Franzens-Universität Graz, 192 pp.

Holdaway, M.J., 2000. Application of new experimental and garnet Margules data to the garnet-biotite geothermometer. American Mineralogist, 85, 881-892.

Jäger, E., Niggli, E. and Wenk, E., 1967. Rb-Sr Altersbestimmungen an Glimmern der Zentralalpen. Beitrag zur Geologischen Karte der Schweiz, 134, 67 pp.

Koroknai, B., Neubauer, F., Genser, J. and Topa, D., 1999. Metamorphic and tectonic evolution of Austroalpine units at the western margin of the Gurktal nappe complex, Eastern Alps. Schweizerische Mineralogische und Petrographische Mitteilungen, 79, 277-295.

Krenn, K., Fritz, H., Mogessie, A. and Schaflechner, J., 2008. Late Cretaceous exhumation history of an extensional extruding wedge (Graz Paleozoic Nappe Complex, Austria). International Journal of Earth Sciences, 97, 1331–1352. http://dx.doi.org/10.1007/s00531-007-0221-z

Kretz, R., 1983. Symbols for rock-forming minerals. American Mineralogist, 68, 277-279.

Laird, J. and Albee, A. L., 1981. Pressure, temperature, and time indicators in mafic schist; their application to reconstructing the polymetamorphic history of Vermont. American Journal of Science, 281, 127-175. http://dx.doi.org/10.2475/ajs.281.2.127

Leake, B.E., Woolley, A. R., Arps, C.E.S., Gilbert, M.C., Grice, J.D., Hawthorne, F.C., Katio, A., Kisch, H.J., Krivovichev, V.G., Linthout, K., Laird, J., Mandarino, J.A., Maresch, W.V., Nickel, E.H., Rock, N.M.S., Schuhmacher, J.C., Smith, D.C., Stephenson, N.C.N., Ungaretti, L., Whittaker, E.J.W. and Youchzi, G., 1997. Nomenclature of Amphiboles: Report of the subcommittee on amphiboles of the international mineralogical association, commission on new minerals and mineral names. The Canadian Mineralogist, 35, 219-246.

Ludwig K.R., 2003. Isoplot/Ex version 3.0. A geochronological toolkit for Microsoft Excel. Berkeley Geochronological Centre Special Publication, 70 pp.

Matura, A. and Schuster, R., 2014. Geologische Karte der Republik Österreich 1:50000, Blatt 135 Birkfeld. Verlag der Geologischen Bundesanstalt, Wien.

Neubauer, F., 1981. Untersuchungen zur Geologie, Tektonik und Metamorphose des "Angerkristallins" und des E-Randes des Grazer Paläozoikums. Jahresbericht 1980, Hochschulschwerpunkt S15, 2, 114-121, Leoben.

Neubauer, F., 1982. Untersuchungen zur Tektonik und Metamorphose und Stellung des Grazer Paläozoikum-Ostrandes. Jahresbericht 1981, Hochschulschwerpunkt S15, 3, 93-101, Montanuniversität Leoben.

Neubauer, F., 1989. Lithostratigraphie und Strukturen an der Basis der Rannachdecke im zentralen Grazer Paläozoikum (Ostalpen). Jahrbuch der Geologischen Bundesanstalt, 132, 459-474.

Neubauer, F., Dallmeyer, R. D., Dunkl, I. and Schirnik, D., 1995. Late Cretaceous exhumation of the metamorphic Gleinalm dome, Eastern Alps: kinematics, cooling history and sedimentary response in a sinistral wrench corridor. Tectonophysics, 242, 79-98. http://dx.doi.org/10.1016/0040-1951(94)00154-2

Neubauer, F., Hoinkes, G., Sassi, F.P., Handler, R., Höck, V., Koller, F. and Frank, W., 1999. Pre-Alpine metamorphism in the Eastern Alps. Schweizer Mineralogische Petrogrographische Mitteilungen, 79, 41-62.

Oberhänsli, R., Bousquet, R., Engi, M., Goffe, B., Gosso, G., Handy, M., Koller, F., Lardeaux, J.M., Polino, R., Rossi, P., Schuster, R., Schwartz, S., Spalla, I.E., Agard, P., Babist, J., Berger, A., Bertle, R., Bucher, S., Burri, T., Heitzmann, P., Hoinkes, G., Jolivet, L., Keller, L., Linner, M., Lombardo, B,, Martinotti, G., Michard, A., Pestal, G., Proyer, A., Rantisch, G., Rosenberg, C., Schramm, J., Sölva, H., Thöni, M. and Zucali, M., 2004. Metamorphic structure of the Alps 1:1, 000,000. Commission of the Geological Map of the World, Paris.

Perchuk, L., 1991. Progress in Metamorphic and Magmatic Petrology. Cambridge University Press, Cambridge, 503 pp. http://dx.doi.org/10.1016/0016-7037(92)90074-S

Purdy, J.W. and Jäger, E., 1976. K-Ar Ages on Rock-Forming Minerals from the Central Alps. Memorie degli Instituti di Geologia e Mineralogia dell'Universitá di Padova, 30, 32 pp.

Rantitsch, G., Sachsenhofer, R., Hasenhüttl, C., Russegger, B. and Rainer, T., 2005. Thermal evolution of an extensional detachment as constrained by organic metamorphic data and thermal modelling: Graz Paleozoic Nappe complex (eastern Alps). Tectonophysics, 411, 57–72. http://dx.doi.org/10.1016/j.tecto.2005.08.022

Röggla, M., 2007. Petrographie und Petrologie des Anger Kristallins, Steiermark. Diploma thesis, Karl-Franzens-Universität Graz, 168 pp.

Russegger, B., 1996. Niedrigst- bis niedriggradige Metamorphose im südlichen Grazer Paläozoikum (Ostalpen). Jahrbuch der Geologischen Bundesanstalt, 139/1, 93-100.

Schaflechner, J., 2002. Geologische und petrologische Aspekte am Ostrand des Grazer Paläozoikums (Naintsch). Diploma thesis, Karl-Franzens-University Graz, Graz, 115 pp.

Schantl, P. and Brandner, K., 2013. Petrologische und strukturgeologische Untersuchungen am Ostrand des Grazer Paläozoikums und im angrenzenden Ostalpinen Kristallin. Bachelor thesis, Karl-Franzens-Universität Graz, Graz, 125 pp.

Scharbert, S., 1990. Rb-Sr Daten aus dem Raabalpenkristallin. In: P. Peindl, F. Neubauer, G. Moyschewitz, H. Reindl, and E. Wallbrecher (eds.) Die geologische Entwicklung des südlichen Raabalpen- und Wechselkristallins, Excursion guide TSK III Excursion "Raabalpen- und Wechselkristallin". Geologisches Institut der Universität Graz, Graz, 22-25.

Schmid, S.M., Fügenschuh, B., Kissling, E., and Schuster, R., 2004. Tectonic map and overall architecture of the Alpine orogen. Eclogae Geologicae Helvetiae, 97, 93–117. http://dx.doi.org/10.1007/s00015-004-1113-x

Schuster, R. and Frank, W., 1999. Metamorphic evolution of the Austroalpine units east of the Tauern Window: indications for Jurassic strike slip tectonics. Mitteilungen der Gesellschaft der Geologie- und Bergbaustudenten in Österreich, 42, 37-58.

Schuster, R., Scharbert, S., Abart, R. and Frank, W., 2001. Per-

mo-Triassic extension and related HT/LP metamorphism in the Austroalpine–Southalpine realm. Mitteilungen der Gesellschaft der Geologie- und Bergbaustudenten in Österreich, 45, 111-141.

Schuster, R., Koller, F., Hoeck, V., Hoinkes, G. and Bousquet, R. 2004. Explanatory notes to the map: Metamphic structure of the Alps, Metamorphic evolution of the eastern Alps. Mitteilung der österreichischen Mineralogischen Gesellschaft, 149, 175-199.

Schuster, R., Schantl, P., Ilickovic, T., Moshammer, B., Krenn, K., Puhr,B., Brandner, K., Proyer, A., Richoz, S., and Hoinkes, G., 2014. PANGEO Austria. Excursion 4. Grazer Paläozoikum und Ostalpines Kristallin im Bereich nördlich von Weiz: Neues zur Tektonik und Lithostratigraphie. Berichte des Institutes für Erdwissenschaften, Karl-Franzens-Universität Graz, 20/2, 73-75.

Schwinner, R., 1925. Das Bergland nordöstlich von Graz. Sitzungsberichte der Akademie der Wissenschaften Wien, 134, 219–276.

Schwinner, R., 1935. Zur Geologie von Birkfeld. Mitteilungen des naturwissenschaftlichen Vereins für Steiermark, 72, 67-100.

Spear, F.S. and Kimball, K.L., 1984. Recamp – A Fortran IV program for estimating Fe3+ contents in amphiboles. Computers in Geology and Geosciences, 10, 317-325. http://dx.doi.org/10.1016/0098-3004(84)90029-3

Spear, F.S., 1993. Metamorphic Phase Equilibria and Pressure-Temperature-Time-Paths. Mineralogical Society of America, Washington D. C., 799 pp. http://dx.doi.org/10.1180/minmag.1996.060.403.17

Sölva, H., Grasemann, B., Thöni, M., Thiede, R. and Habler, G., 2005. The Schneeberg Normal Fault Zone: Normal faulting associated with Cretaceous SE-directed extrusion in the Eastern Alps (Italy/ Austria). Tectonophysics, 401, 143-166. http://dx.doi.org/10.1016/j.tecto.2005.02.005

Thöni, M., 2006. Dating eclogite-facies metamorphism in the Eastern Alps - approches, results, interpretations: a review. Mineralogy and Petrology, 88, 123-148. http://dx.doi.org10.1007/s00710-006-0153-5

Tollmann, A., 1963. Ostalpensynthese. Deuticke, Wien, 256 pp.

Tröger, W.E., Bambauer, H.U., Taborszky, F., and Trochim, H.D., 1982. Optische Bestimmung der gesteinsbildenden Minerale. Schweizerbart'sche Verlagsbuchhandlung, Stuttgart, 822 pp.

Tropper, P., Bernhard, F. and Konzett, J., 2001. Trace element mobility in contact metamorphic rocks: Baddeleyite-Zirconolite-(Zircon) veins in olivine-bearing marbles from the Stubenberg Granite Contact Aureole (Styria, Austria). Journal of Conference Abstracts, 6, 1, p. 278.

Received: 19 February 2015
Accepted: 24 July 2015

Philip SCHANTL[1)*)], Ralf SCHUSTER[2)], Kurt KRENN[1)] & Georg HOINKES[1)]

[1)] Institute of Earth Sciences, University of Graz, Universitätsplatz 2, A-8010 Graz, Austria;

[2)] Geologische Bundesanstalt, Neulinggasse 38, A-1030 Wien, Austria;

[*)] Corresponding author, philip.schantl@edu.uni-graz.at